Physics – Uspekhi **63** (2) 103 – 122 (2020)

REVIEWS OF TOPICAL PROBLEMS PACS numbers: **07.78.+s**, 42.65.Re, 61.05.J–

Structural dynamics of free molecules and condensed matter

S A Aseyev, A S Akhmanov, G V Girichev, A A Ischenko,
I V Kochikov, V Ya Panchenko, E A Ryabov

DOI: https://doi.org/10.3367/UFNe.2018.11.038477

Contents

Abstract. Advances in the development of pulsed lasers provided a further breakthrough in the study of the structural dynamics of nuclei and electrons. As a result of this progress, the use of powerful femtosecond laser pulses, both for exciting a sample and for generating ultrashort (down to femto- and even subfemtosecond) photoelectron bunches synchronized with optical pulses for sensing matter, made it possible to observe the coherent dynamics of nuclei and electrons in samples at the required spatiotemporal scales. The possibility of direct observations of reaction processes is a major breakthrough in chemical physics. The many-particle potential is so complex that the degree of the interaction nonadiabaticity cannot be determined with an accuracy sufficient for predicting reaction paths. How can this information and a new look at the reaction dynamics be used in the future? This question arises in connection with the development of a new conceptual foundation of natural sciences incorporating the convergence of experimental and theoretical tools in studies of systems of any complexity with atomic resolution. In this approach, an 'atomic–molecular' movie is obtained by using mutually complementary information extracted from simultaneous studies of ultrafast electron (or X-ray) diffraction, spectroscopy, and the quantum dynamic theory of matter.

Keywords: ultrafast structural dynamics, ultrafast electron diffraction and microscopy, femtosecond laser radiation, electron beams of ultrashort duration

In memory of V N Bagratashvili
(01.03.1947–12.04.2018)

> "If there is simplicity somewhere in physics and chemistry, it is not in microscopic models. It lies more in idealized macroscopic representations, for example, concerning simple motions of the harmonic oscillator type or a problem of two bodies. But, when such models are applied to describe the behavior of large or very small systems, the simplicity proves to be irrevocably lost. And as soon as we lose the faith to the simplicity of the microscopic approach, the only way out remaining for us is to introduce properly time again."
>
> I Prigogine, *From Being to Becoming: Time and Complexity in the Physical Sciences* (Moscow: Nauka, 1985) p. 11

1. Introduction

Chemical physics, by definition, includes the structural dynamics of matter during the transformation of molecules. The dream of every researcher is the direct real-time observation of the motion of atoms and molecules during a chemical reaction. In the 1980s, researchers at various scientific laboratories around the world began to develop a new field of studies — structural dynamics in real time and the creation of a 'molecular cinema' for visualization of the motion of nuclei and electrons in molecules. The experimental observation of the behavior of matter in the spatiotemporal continuum at ultrashort scales is the first necessary step for explaining and controlling nonequilibrium processes and operating the systems under study, which

S A Aseyev [1,*], **A S Akhmanov** [2], **G V Girichev** [3], **A A Ischenko** [4], **I V Kochikov** [5], **V Ya Panchenko** [2], **E A Ryabov** [1]
[1] Institute of Spectroscopy, Russian Academy of Sciences, ul. Fizicheskaya 5, 108840 Troitsk, Moscow, Russian Federation
[2] Federal Scientific Research Center "Crystallography and Photonics", Russian Academy of Sciences, Leninskii prosp. 59, 119333 Moscow, Russian Federation
[3] Ivanovo State University of Chemistry and Technology, prosp. Sheremetevskii 7, 153000 Ivanovo, Russian Federation
[4] MIREA — Russian Technological University, prosp. Vernadskogo 78, 119454 Moscow, Russian Federation
[5] Lomonosov Moscow State University, Scientific Research Computer Center, Leninskie gory 1, Building 4, 119991 Moscow, Russian Federation
E-mail: [*] aseyev@isan.troitsk.ru

Received October 4, 2018, revised November 19, 2018
Uspekhi Fizicheskikh Nauk **190** (2) 113 – 136 (2020)
Translated by M Sapozhnikov; edited by A M Semikhatov

allows analyzing interrelations among the elements of the structure–dynamics–properties triad [1].

The expression 'creation of a molecular cinema' refers to recording the relative atomic motion of complex many-particle nonlinear systems in the three-dimensional Cartesian space rather than the construction of a multidimensional landscape of the potential energy. This 'thought experiment' was previously assumed to be beyond the field of experimental science, simply remaining a mental construct, useful in developing basic concepts in the natural sciences. In recent years, the required technology has been developed to such an extent that this dream is becoming true, as is shown in this review.

The prospects for achieving the spatiotemporal resolution required for the direct observation of atomic motion were dim. The necessity and efficiency of methods based on rapid perturbations of systems (perturbative methods) for studying the dynamics of reactions were probably first demonstrated by Eigen [2]. The development of this field resulted in great progress in combining spectroscopy with different variants of molecular-beam methods for constructing reaction diagrams. For his studies of 'unmeasurably fast reactions', Eigen was awarded the Nobel Prize in Chemistry in 1967 [2]. However, this approach proved to be successful only for simple molecular systems. In addition, such measurements can only identify certain subsets of reaction modes (which can be analyzed by spectroscopic methods) but cannot give the displacements of atoms along all coordinates, which is the most important information. Ahmed Zewail, the Nobel Prize Laureate in Chemistry in 1999 [3], who analyzed reactions a billion times faster in time than did Eigen, later joked about the term 'unmeasurably fast reactions' [4]. It is clear at present that if the methods of attosecond physics do become an accessible tool in scientific laboratories, the term 'unmeasurable' will have to be redefined once again.

Attosecond technology [5] drastically improved the time resolution of time-resolved spectroscopy of ultrafast phenomena. This technology revealed the richness of ultrafast microscopic phenomena caused by the motion of electrons, which could not be observed earlier [5]. Conceptual and experimental achievements that laid the foundation for the birth of attosecond science showed the fundamental necessity of progress in many fields for realizing such a revolution in technology. The current revolution in science or technology is based on progress in numerous scientific areas, which in turn depends on the cooperation of researchers from different fields (and on their skills and persistence). Characteristic spatiotemporal scales in atoms, molecules, nanostructures, and solids are presented in Fig. 1.

At present, a number of dynamic structural studies of free molecules in condensed state are performed using the methods of ultrafast electron diffraction, crystallography, and microscopy. These investigations include studies of the coherent dynamics of nuclei, from simple molecules and atomic crystals to complex biological objects (see reviews [1, 6–17] and monographs [18–21]).

The main problem is to understand the generalized principles that allow reducing the control of chemical reactions to several key modes and to apply these principles for predicting reactions of different classes. The aim of studies is to find the interrelation between the main elements of the structure–dynamics–function triad, which should lead to a new level of understanding and controlling some physicochemical, chemical, and biochemical processes. To achieve

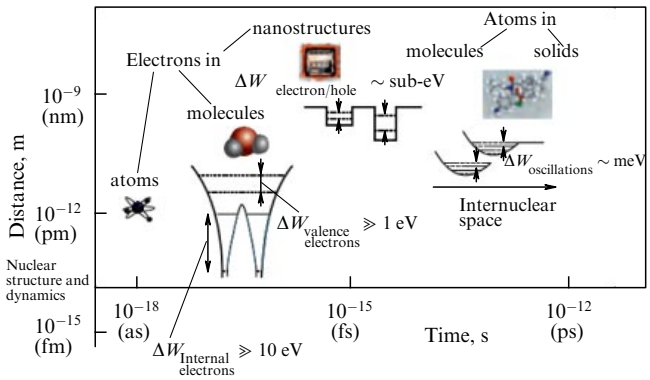

Figure 1. Characteristic spatiotemporal scales in the subatomic world [5].

this goal, it is necessary to study not only the structural dynamics of initial substances and intermediate (transient) states but also the entire chain of transitions (molecular cinema) [6, 11, 16].

In this review, we discuss the main areas in the development of the experimental techniques of ultrafast electron diffraction and electron microscopy, aimed first and foremost at the increase in the brightness of a structural probe. We show that to obtain a sufficiently complete picture of the structural dynamics of molecules and condensed matter, it is necessary to analyze the results obtained by different spectroscopic and diffraction methods based on different physical phenomena supplemented by quantum mechanical calculations of the dynamics of molecular systems.

2. Experimental technique

Today, three main areas can be distinguished in the development of the experimental technique of ultrafast electron diffraction aimed at obtaining a femtosecond time resolution (potentially, considerably shorter than 100 fs). The first is the use of relativistic electron beams in combination with the radiofrequency compression technique (the accelerating voltage is ~ 5 MV, with $10^6 - 10^8$ electrons in a pulse less than 100 fs in duration). The second is the use of 30–200 keV one-electron probe bunches with high pulse repetition rates about 1 MHz and a long diffraction signal accumulation time. The third is a temporal lens and the nonorthogonal intersection of the wave front of exciting optical and probe electron pulses: the diffraction of low-intensity nonrelativistic ultrashort electron pulses with a high pulse repetition rate and the inclined geometry of intersection of the wave front of electron and laser pulses providing a subfemtosecond synchronization accuracy of pulses. The development of the technology of generating ultrashort ultrabright electron pulses opens the possibility of observing the motion of atoms at the initial time scales of barrier crossing, which is fundamentally important for optimizing the mechanisms of chemical reactions.

3. Evolution of electron source brightness: potential to observe the reaction dynamics with atomic resolution

Pulsed electron sources bright enough to 'illuminate' atomic motion have become a key technology for solving the main problem in experimental chemical physics. The path to this achievement began with relatively low-intensity electron

beams and was developed simultaneously with the improvement in light sources for spectroscopy. In 1980, the first experiments were performed that laid the foundation for the methodology and technique of studying the dynamics of chemical reactions with atomic resolution [22, 23]. The dynamics of chemical reactions were studied by the laser pump–probe method using an electron probe pulse as a structural probe. A set of deflection plates controlling the electron beam in experiments provided nanosecond time resolution, which was already sufficient for determining the structures of transient intermediate compounds in the photochemistry of CF_3I. This work demonstrated the use of electron probes in studying the intermediate compounds of photoinduced reactions.

The next important event in studying the coherent structural dynamics was the use of pulsed photoelectron sources (rather than continuous electron sources modulated by deflection plates) [24, 25]. Using this approach, Zewail's group was the first to achieve the time resolution of a few picoseconds [3, 10]. In view of the low signal-to-noise ratio for gas-phase electron diffraction experiments, these achievements [3, 10, 22–25] are all the more remarkable for studying the structures of intermediate compounds. This pioneering work established a standard still used in gas-phase photochemistry. However, the time resolution limited by the duration of electron pulses and the mismatch between laser excitation and the electron probe in experiments was sufficient only for studying intermediate structures and insufficient for observing the correlated motion of atoms leading to intermediate reaction products.

The first experiments in which a subpicosecond time resolution was achieved using quite bright pulsed electron beams were performed at Miller's laboratory [11, 14, 16]. The authors for the first time recorded the relative motions of atoms during melting caused by high-power laser radiation. The 600 fs time resolution achieved in these experiments revealed the motion of atoms resulting in the dissociation of chemical bonds. The time resolution remained high even when the electron source was intense enough to provide single measurements. The most important feature of these studies was the understanding that the analysis of irreversible processes requires an electron source with brightness sufficient for one-shot measurements [11].

The time resolution of experiments is critically important in studies of the structural dynamics. However, there is great confusion in the literature when the accent is often placed only on the electron pulse duration and the use of completely reversible processes to demonstrate the time resolution. The brightness of probe electron pulses is then disregarded; as a result, a discussion of the potential of the method exclusively in terms of the electron pulse duration distracts from real measurement problems, such as image reconstruction with all the ensuing tasks of achieving the brightness sufficient for reliably obtaining the Fourier components and an accurate image reconstruction. In the final analysis, the electron source brightness is a very important characteristic [17].

To fully estimate the role of this parameter in visualizing atomic-resolution dynamics, we consider elements required for the construction of an experimental setup to record molecular movies. We first consider the image (illumination) source requirement for achieving the spatial resolution needed to observe the paths of chemical reactions. To resolve vibrational nonadiabatic coupling with reaction coordinates and the effect of vibrational anharmonicity, a subangstrom spatial distribution is required. For example, carbon atoms involved in the primary event of the visual process — the photoisomerization of 11-cis-retinal to the complete *trans-form* — move by 0.1 Å [14, 16]. Therefore, the wavelength of diagnostic radiation should be about 0.1 Å or shorter. Using diffraction methods, this requirement can be satisfied with the help of hard X-rays or high-energy electrons.

We now discuss the time resolution requirements. The corresponding 'gate' rate can be estimated from the time during which two atoms (or the reduced masses) move along the dissociation coordinate to the point where the binding energy is no longer within the thermal energy range kT. At this moment, corresponding to a certain value of the reaction coordinate, the chemical bond dissociates. For typical rates $\sim 10^3$ m s^{-1} determining thermal fluctuations and potential energy surfaces requiring a displacement of about 1 Å to reach the disconnected parts of the potential, the corresponding time scale is 100 fs. This is a typical discretization rate of the Arrhenius equation for the rate of a first-order reaction. Despite the simplifications, the estimate gives relevant time scales. There are faster dissociative channels involving excited states with lifetimes about 25 fs [14, 16], but most of the chemical reactions are related to the long-range correlated motions of collective modes, especially in a condensed phase, where the most strongly decaying modes along the reaction coordinate are in the range from 100 to 10 cm^{-1} ($>$ 100 fs) [14, 16].

The fastest chemical process not resulting in dissociation and related to photoinduced isomerization accompanied by internal rotation about the double bond of the $C_{11}-C_{12}$ fragment is the primary stage of vision. This process was initially assumed to develop at the 200 fs time scale. At present, it is established that the primary vision process occurs by mixing all three key modes at the 30 fs time scale [14]. This is one of the most highly optimized known chemical processes, especially if we take the scale of the biological system into account. All the other chemical processes typically proceed more slowly, and hence the 100 fs time scale is a useful metric for the required time resolution. We note, however, that faster nuclear motions do exist.

Faster nuclear motions are valence vibrations of the OH groups of water with a half-period of 10 fs. However, the root mean square displacement of atoms in this case is smaller than 0.05 Å, this value being insignificant compared to displacements related to barrier crossing processes. This is the time scale of nuclear fluctuations during which the coupling of different vibrational modes leads to the highly anharmonic localized motion of nuclei through a barrier, a process that underlies chemical reactions. This occurs mainly at the 100 fs time scale [16]. The thermal capacity or a thermal reservoir responsible for nuclear motion producing a chemical reaction is determined to a greater extent by the internal energy of the system within nuclear degrees of freedom. This fact partially explains the success of the Born–Oppenheimer approximation used to describe the dynamics of molecular wave functions. The only moment when the electron dynamics become slower than the nuclear dynamics concerns conical intersections, where mixing between electron states is small ($<$ 100 cm^{-1}) [14, 16]. However, even here, the nuclear motion brings the system to the barrier-crossing region and determines the time scale of the evolving process. The electron dynamics at such nuclear configurations determine the quantum efficiency rather than the effective time scale of barrier crossing.

We here use the 100 fs time scale as the canonical time resolution required for the atomic resolution of the dynamics of chemical reactions. No detector has a time response sufficient to resolve the structural molecular dynamics at this time scale. The system under study must first be excited so as to initiate structural changes and then a structural probe is to be used in a repeating gated pump–probe regime by successively recording the frames of a movie showing the motion of atoms, as was first proposed in [22, 23]. This approach is currently the standard for femtosecond pump–probe spectroscopy.

A slow detector is used to record the probe intensity for each time delay. The main problem in the past was to generate pulses short enough for studying the time-resolved dynamics of the process. It was necessary to generate sufficiently short X-ray or electron pulses to record the corresponding motion. The 100 fs time scale may seem extremely fast for X-rays or electron excitation sources, but well-known methods exist using either a laser plasma or laser-induced emission to generate short enough X-ray or electron pulses. The real problem is the source brightness.

The required source brightness was achieved only 20 years after the advent of the first femtosecond lasers. This problem can be easily understood by analogy with a film camera. Because the aim is to attain progressively higher gate rates (time resolution), maintaining the image quality requires progressively brighter sources. The image quality depends on its contrast, which is related to the dynamic range of recording, which in turn depends of the brightness or the integrated detected flux from the image source. This problem was a driving force for the development of faster shutters and flashlamps at the dawn of photography for motion 'freezing'.

Brightness determines the signal-to-noise ratio (SNR) and gradients of the image contrast. To understand this problem, we discuss the visualization method. Structures can be obtained with atomic resolution by the diffraction method (reciprocal space) or by visualization in real space. The diffraction signal increases as N^2, while visualization in real space scales as N, where N is the number of unit cells in a crystal sample volume [14–16]. For this reason, diffraction scales in experiments quadratically with the sample thickness, or as N^2. This amplification coefficient makes the diffraction regime an order of magnitude more sensitive than visualization in real space and is now the only option for the real-time visualization of atomic motions.

For simple unit cells (containing about 10 atoms per cell), the number of detected electrons needed to achieve a sufficient number of diffraction orders with a dynamic range providing a detailed resolution of corresponding motion is of the order of 10^4 and increases approximately linearly as the number of atoms in the unit cell increases. There is an empirical rule for forming a representative sample: 10^5 electrons are required for typical molecular systems having ~ 100 atoms per unit cell and 10^7 electrons are required for comparable systems with proteins. This scaling can be obtained by analyzing typical static diffraction patterns. A genuine problem with the source brightness appears because of the necessity to photoinitiate the structural dynamics of interest.

A single chemical transformation event, or a structural transition, rarely occurs exclusively in an equilibrium system and must be photoinitiated to fix the time the process starts, $t = 0$. To obtain a signal above the background, about 10% of the sample volume must be excited. This requires high power densities of the exciting radiation. Because photochemical reactions initiated by high-power laser radiation are usually irreversible, excitation even by a single high-power laser pulse causes damage to the sample. This important circumstance must be taken into account.

The preparation of high-quality samples 10–100 nm in thickness for electron-beam studies in the transmission regime is an extremely complicated problem. Even if we study only completely reversible systems, samples of this thickness require 10–100 ms to recover. As a result, the signal repetition rate decreases to 10 Hz or less, and an adequate signal-to-noise ratio in the image of atomic motion requires an increase in the accumulation time, which increases quadratically, to obtain a sufficient signal. The lifetime of irradiated samples is limited, and hence brighter sources provide better resolution and contrast of the atomic motion pattern. In addition, the requirements for 100 fs time resolution and the radiation pulse energy necessary to obtain the desired fraction of excited states lead to minimal peak laser radiation powers of the order of 10–100 GW cm^{-2}. Peak laser radiation powers in this range cause damage to the samples, which only highlights the need in probe brightness capable of generating electron or X-ray pulses with intensities sufficient for determining the structure in the single-pulse regime.

All the technologies available in the 1980s–1990s could be used in ultrafast electron diffraction experiments only with low-brightness electron sources. The brightness problem was solved only recently [14–17]. We note that it is insufficient to simultaneously have high spatial and time resolutions (femtosecond excitation and femtosecond pulses from a structural probe); to follow the chemical reaction, the structural probe should have a brightness sufficient for determining the structure by a single pulse. In some cases, photoreversible processes alleviate this condition, but thermal effects usually determine the pulse repetition rate, which makes the requirement for high brightness of sources the general condition [16, 17].

The brightness of an electron source is mainly limited by the Coulomb repulsion between electrons, which limits the charge density in a pulse for the specified energy or brightness distribution. We note that this limitation, which, as was assumed earlier, could not provide the atomic resolution required to observe the structural dynamics, stimulated the application of X-ray free electron lasers (XFELs) for solving such problems.

Considerable progress in increasing the electron source brightness was achieved by exactly solving the coupled equations of motion for an ensemble of 10^4 electrons to imitate the propagation dynamics of an electron bunch, providing the recording of a diffraction pattern for a single pulse [14–17]. Calculations revealed a very strong pulse elongation, which, however, did not greatly impair the spatial coherence or the resolving power when the required electron densities were used, especially if the electron beam propagated over a short distance to the scattering region. The unexpected conclusion was that no considerable losses in the spatiotemporal correlation were observed under these conditions. Electrons at the pulse front are accelerated to higher velocities with respect to the lagging electrons, which are similarly decelerated to lower velocities. For nonrelativistic electrons, this leads to the self-sorting of electron energies, with the electron pulse acquiring an almost perfect linear

chirp.[1] (We note that this feature was ignored in previous analytic methods used to solve the problem.) It follows from the cited papers that such linearly chirped electron pulses can be easily recompressed in the sample region.

An alternative and most reliable solution, also presented in [14–17], was the use of extremely compact electron guns to minimize pulse broadening by restricting the propagation length of the electron bunch. This study is crucially important because it yields information on experimental parameters required for the construction of a compact electron gun with a sufficient number of electrons and coherence for determining the structure with a single pulse without electron bunch compression [14–17], which considerably simplifies the electron gun design. Currently, determining structure with a single pulse has become possible even for complex systems [14–17]. Modern photoelectron guns can generate 100 fs pulses with a beam diameter of 100 μm containing up to 10^5-10^6 electrons, which corresponds to typical laser pulse profiles [10, 16].

4. Triunity of the spectral, diffraction, and quantum chemical methods for studying the ultrafast structural dynamics of matter

Currently, a major part of the results from studies of intermediate compounds and the dynamics of chemical reactions are those obtained with the help of light rather than electrons or X-rays. These results were obtained by different spectral methods.

The history begins with flash photolysis, discovered in the late 1940s–early 1950s (see [26]), which received wide acceptance and recognition (Nobel Prize in Chemistry, 1967). Even with the use of classical light sources, pulsed lamps, this method provided the identification of intermediate products of photoinduced reactions with a submicrosecond time resolution.

With the advent of lasers generating short light pulses tunable in a broad frequency range, many different methods of laser spectroscopy were developed for studying dynamic processes with femtosecond and attosecond time resolution. We do not consider these methods in detail here: they are described by many authors in the literature. In particular, a description of these methods and their applications can be found in book [23] and review [28]. Here, we briefly consider only a number of questions directly related to the topic of this review: relaxation processes and the intramolecular dynamics of molecules in the ground electronic state.

The advent of pulsed tunable IR lasers has allowed studying processes occurring under excitation of vibrational states of molecules, i.e., under direct excitation of their nuclear subsystem. First and foremost, this considerably advanced the study of collisional relaxation of vibrational excitations: V–V exchange and V–T/R relaxation (see reviews [28, 29]). The use of multiphoton IR excitation (MPIRE) of molecules (see monograph [30]) allowed studying relaxation processes in highly excited molecules. In particular, it was shown in [31] that the rate of vibrational–translational (V–T/R) relaxation is a nonlinear function of the excited vibrational level of molecules. Multiphoton IR excitation was used to study intramolecular vibrational redistributions (IVRs) [30–33]. In [34], the energy stochastization boundary of the vibrational energy in molecules was discovered. Later, with the advent of lasers emitting ultrashort pulses, methods of IR and Raman spectroscopy were used to study IVR dynamics with pico- and femtosecond time resolution. The results obtained in these studies are presented in detail in review [35].

By exciting *vibronic* states, in particular, in a simple diatomic molecule, a spectral signal reflecting the dynamics of a wave packet can be related to the dynamics of the molecular structure. The situation becomes complicated when the number of atoms increases, and the extraction of information on the structural dynamics becomes a difficult problem even for simple polyatomic molecules consisting of several atoms. This occurs because optical spectroscopy probes valence electronic states related to many parts of the molecular system; hence, they are only indirectly and ambiguously related to the dynamics of the nuclear subsystem. An exception is provided by some favorable cases that can be studied by the methods of vibrational spectroscopy [36–41] and coherent multidimensional spectroscopy [42–44]. Therefore, alternative or additional methods providing the extraction of direct dynamical structural information are required. In particular, XAFS (X-ray Absorption Fine Structure) methods are often used to study the fine structure of the X-ray absorption spectrum in the vicinity of the absorption jumps of elements contained in the sample [45, 46].

It is known that X-ray absorption spectra have sharp absorption edges (a sharp increase in absorption), called absorption jumps. Photons with energies slightly exceeding the absorption edge energy can ionize the inner shells of atoms/ions of matter, generating photoelectrons with a certain energy. The photoelectrons propagating in the vicinity of a resonantly absorbing atom (i.e., with a jump caused by the creation of a photoelectron) are scattered by the electron shells of atoms and ions and after relaxation give information on the number of neighboring atoms and their distance to the reference atom. This information is manifested in the specific wavy shape of the absorption spectrum in the range of ±40 eV with respect to the absorption jump energy and extending by approximately 1000 eV beyond this region. This is called the XAFS spectrum [45, 46]. Having a theory describing the X-ray photoeffect from the absorption of a photon to the relaxation of the excited atom, it is possible to refine the model of the process, taking the mutual arrangement of scattering atoms with respect to the absorbing atom into account, i.e., to determine the nearest-order structure.

Currently, the XAFS theory is well developed and widely used for the structural analysis of matter based on the fine structure of absorption spectra [45, 46]. Even a brief description of the XAFS method shows that the measurement of detailed absorption spectra by this method in a range of about 1000 eV requires the use of a specific probe — an X-ray beam with a broad continuous spectrum or with a spectrum precisely controlled in a broad energy range. Synchrotrons, which became available to researchers in the early 1970s, proved to be the most suitable radiation sources for such measurements. Afterwards, the XAFS theory and applications of this method for structural analysis were rapidly developed [45, 46].

Although XAFS methods can be used only to study the nearest-order structure at distances not exceeding the free path of a photoelectron in a sample, they are very attractive for material engineers, first, because they are applicable for studies of materials in any aggregate state and, second, due to

[1] A chirp is a temporal variation in the phase of an electromagnetic wave.

the simplicity of measurements, which, as a rule, do not require complex goniometers and vacuum systems. It suffices to have a sample holder and point detectors measuring the X-ray beam intensity in front of and behind the sample.

The EXAFS (Extended X-ray Absorption Fine Structure) signal distribution can be used to calculate characteristics of the signal, such as the distribution $g_{\alpha\beta}(r)$ of pairs of α and β atoms of the system in direct space. If the function $g_{\alpha\beta}(r)$ or the combination of partial functions $G_\alpha(r)$ for particular α atoms or ions or even full functions $G(r)$ for all elements in a liquid are known, they can be used to determine interatomic distances, coordination numbers, and the degree of local order around a chosen atom. The analysis of the near-threshold region by the XANES (X-ray Absorption Near Edge Structure) method considerably differs from the EXAFS analysis.[2] The XANES spectra can be sensitive to oxidation states [45, 46].

Analysis of EXAFS data can give information on the local environment of a chosen atom, i.e., the type, number, and distance from backscattering atoms around a resonantly absorbing reference atom. We note that scattering atoms are not necessarily chemically bonded to the absorbing atom. The distance measurement error in this method is usually about $\pm 1\%$ within the radius of 6 Å. However, the error in the measurement of the coordination number strongly depends on the system under study and can be large. For this reason, the EXAFS results should be compared with data obtained by other methods. Because the observed fine structure is related to the absorption edge of one particular type of atoms and the absorption edge energy depends on the chemical element and its oxidation degree, the EXAFS method is used to study the local structure around a given particular element in a given oxidation state. But studying several absorbing elements in a sample allows obtaining a more complete and reliable picture of the sample structure [45, 46].

Because the EXAFS and XANES methods give local structural information [45, 46], a signal can be obtained under local laser excitation.

The EXAFS method provides quantitative information about the structure with a subangstrom resolution with the help of the so-called EXAFS equation [47], whereas XANES provides quantitative information, 'fingerprints,' related to the local geometry of a chemical bond and the orbital hybridization in the vicinity of the atom (atoms) of interest [46]. This can be useful for understanding the molecular dynamics in solutions where the solvent considerably affects the dynamics of the chemical reaction.

Similarly to time-resolved X-ray diffraction in liquids [48, 49] (time-resolved X-ray liquidography, TRXL), X-ray absorption spectroscopy was used in time-resolved studies. A scheme with a pump laser and an X-ray probe was used to study the charge transfer [47, 50–54] and spin crossover [55, 56] in the chemistry of coordination compounds, the solvation dynamics of radicals [57], and the structural dynamics of the intermediate compounds of photodissociation in the liquid phase [54, 58]. The structural information obtained from X-ray absorption is restricted by the local environment of a particular atom, which is in contrast to diffraction methods, where the diffraction signal contains information on all the particles located in the scattering region. However, this is a specific advantage of the EXAFS and XANES methods, because the local absorption of X-rays provides higher sensitivity. The TRXL method and time-resolved X-ray absorption spectroscopy supplement each other well, and a combination of these methods in the future can be useful for obtaining more complete and reliable information on the structural dynamics in solutions.

The time resolution of the TRXL is currently limited by the duration of X-ray synchrotron radiation pulses (~ 100 ps). The resolution can be considerably improved in the next generation of radiation sources such as XFELs and LINACs (LINear ACcelerators), which can generate almost completely coherent subpicosecond X-ray pulses with high photon flows. Recently, using XFELs, a time resolution of 67 fs was achieved (https://www-ssrl.slac.stanford.edu/stohr/xfels.pdf). It thus became possible to study the motion of atoms along the potential energy surface, the formation and dissociation of chemical bonds, and isomerization in the liquid phase in real time. However, when such short X-ray pulses are used, the assumption about the thermal equilibrium of a dissolved substance and hydrodynamic equations used for a solvent are violated [49]. Therefore, it is necessary to develop new theoretical methods to analyze the TRXL data for studying the ultrafast structural dynamics. When these problems are solved, TRXL will have a great effect on dynamical studies of chemical reactions in the condensed phase.

The replacement of an optical probe by an X-ray [45, 59–75] or an electron diagnostic pulse opens a direct way to study the molecular structure dynamics, because diffraction (scattering) is produced by an ensemble of atoms in real space, rather than by optical resonances in the energy space. Unlike visible or infrared radiation exciting electronic or vibrational transitions of chromophore groups, X-rays and electrons diffract (or are scattered) from all atoms and atom–atom pairs. This scattering contains direct information about the molecular structure, which can be obtained by solving the inverse structural problem for time-dependent X-ray and electron diffraction data. For example, most 3D protein structures were determined with the help of X-ray crystallography. The diffraction of pulsed X-ray beams excited by synchronized laser pulses can be used to study the structural dynamics of proteins.

X-ray free-electron lasers are sources of self-amplified spontaneous emission (SASE) and have 100% variability. The root-mean square amplitude instability, time-averaged over several-minute intervals (30–100 Hz), is 5–12%, while the corresponding wavelength instability is 0.1% for an energy instability of 0.1% [59], which affects the image quality in diffraction. This stability is to be compared with the stability of electron sources replicating the amplitude stability of a solid-state laser used for photoinjection. Here, the root-mean square amplitude stability is 0.1% for the same integration time and the energy stability is $< 10^{-5}$.

In fact, the shorter wavelength of electrons also provides a much higher spatial resolution than do usual X-rays (obtained for a 10 kV accelerating voltage). However, the

[2] The difference between the EXAFS and XANES methods is clearly illustrated by considering the de Broglie wavelength λ_D for photoelectrons produced by irradiating a material with X-rays. When the quantum energy slightly exceeds the absorption edge for the given chemical element, the energy of the produced photoelectrons is small, and λ_D is, correspondingly, large and can exceed the characteristic distance between atoms in the sample (XANES). In this case, it is necessary to take multiple scattering of photoelectrons by the environment into account. In another limit case (EXAFS), when the de Broglie wavelength becomes small compared to the characteristic distance between atoms, it is sufficient in the first approximation to take only single scattering into account.

disadvantage is that the preparation of samples for electron diffraction measurements is considerably more complicated than for X-ray measurements. Samples should have a thickness of about 100–200 nm or smaller (depending on their composition, the element number Z, and the electron energy) to avoid multiple scattering in diffraction and should have a surface area sufficient for accumulating the number of temporal points required to solve the structural dynamics problem. This difference is the main advantage of XFELs, especially in studies of biological systems, where protocols for the preparation of large-area thin crystals are not yet developed. At present, XFELs are the only source providing atomic resolution of the dynamics in biological systems for solving a number of key problems of the interrelation between the structure and biological functions [45, 60–75]. However, a large class of systems exists that can be studied with the help of electron probes, and the brightness of the electron source is already sufficient for studies of biological systems (see Section 3).

The advent of nanotechnologies and long-term efforts of researchers in the field of electron microscopy made the preparation of thin enough samples for electron probes possible. The solution to the problem of creating and characterizing sufficiently bright electron sources for studying the dynamics of chemical reactions with atomic resolution was crucial. It resulted in the creation of the first atomic–molecular movies of structural dynamics with diffraction orders sufficient for the resolution of key relative atomic motions governing the structural transition at time scales faster than the collisional processes that can blur the details. Now, everything is reduced to the systematic study of different chemical processes. The formation of a sample is the main experimental problem requiring the development of high-brightness electron sources.

We note that the problem of electron spatial charge can also be solved by using beams with a low electron density and hence with an electron gun commonly used in transmission electron microscopes (TEMs) or diffraction setups for gas-phase studies [32, 37 38, 45, 46, 49]. The restriction on the time resolution of the spatial charge should be carefully separated from the general requirements for image reconstruction, as discussed above. In the limit of single-electron pulses, spatial charge effects can be completely removed. The concept of single-electron pulses was proposed as the final solution to the time resolution problem, neglecting the spread of electron bunches propagating in the acceleration gap ($\sim 60-300$ fs). This statement disregards all the details of the reconstruction of an electron diffraction image and the minimal dynamic range required for inverting the diffraction pattern into the real-space image. However, an important advantage of single-electron pulse sources with nanopointed cathodes is that the spatial resolution can in principle be several orders of magnitude better than with flat photocathodes if a high enough SNR can be achieved. In this case, the arbitrarily high transverse coherence can be achieved in principle. However, the accumulation of a sampling sufficient for imaging then becomes the main problem.

To illustrate the limitation of the single-electron approach, we consider the diffraction pattern produced by approximately a million scattered electrons (assuming a 100% efficiency of the detector) for a system with the unit cell in the range of 3–10 nm (for example, a protein system) and a moderate requirement for the spatial coherence of such sources. The sampling (the total number of events) of excitations and probing should then be about 10^8 in order to have 0.01 electrons per photoinjection pulse to generate single electrons without the loss of spatiotemporal coherence from a source 10 μm in size. The spatial resolution for the given SNR for obtaining real-space images is directly related to the number of electrons and approaches even more nonrealistic numbers of excitation events, namely, 10^{15} for a resolution of 1 Å for the sufficient image contrast provided by SNR = 100 [39–41].

Previous discussions of a femtosecond time resolution with the spatial resolution of 1 Å neglected this critical circumstance [41]. The photoreversibility problem was not considered either. At present, samples capable of withstanding about 10^6 photocycles in chemical reactions under the completely reversible conditions required by the single-electron approach are unknown. We recall that the preparation of high-quality samples is the main restriction on transmission electron microscopy, and single-electron approaches will require an exposition an order of magnitude longer than sources providing the atomic resolution for a single pulse.

The number of reversible processes is considerably restricted compared to numerous systems and objects in which photoinduced irreversible processes take place and which can be studied using bright electron sources. In this case, sample heating is a serious problem. Even in the limit of completely reversible systems, the time scale of the complete thermal relaxation between laser pulses limits the pulse repetition rate to 100 Hz to avoid the accumulation of artifacts related to the sample heating, the reproducibility of results, and the time required for sample recovery [39, 40]. These apparently trivial technical details considerably increase the duration of the experiment and the number of probes. As a result, the single-electron approach becomes theoretically possible only for studying reactions in gas flows.

Moreover, as follows from the foregoing, there is no reason to use single-electron pulse sources to study the structural dynamics from the standpoint of corresponding time scales. Modern high-brightness sources have achieved the spatiotemporal resolution required to observe the nuclear dynamics. We note that the prospects of using single-electron sources to study the reaction dynamics are qualitatively similar to the use of single-photon sources in femtosecond spectroscopy. Similarly, spectra with femtosecond resolution could be accumulated by using single-photon pulses, but this would require a 10^8 times longer exposure in usual pump–probe methods (for typical 100 pJ pulse energies) to achieve the same integrated photon flux by recording signals with a considerably lower SNR, taking the higher noise level during a longer data accumulation into account.

The study of the femtosecond dynamics became possible with the help of lasers providing a sufficient photon flux and measurements of small variations in optical properties correlating with the dynamics of the quantum state of the objects under study. At present, no applications of the single-electron approach for studying the chemical kinetics with atomic resolution have been reported. Everything reduces to the sampling accumulation, and only in the limit where spatial or temporal restrictions cannot be removed with the help of bright sources would it be reasonable to use single electrons to study the reaction dynamics with atomic resolution.

However, certain fields exist where single-electron sources have a great advantage. For example, the interesting X-ray

spatial mapping of attosecond electron dynamics was performed in [39]. Single-electron pulse sources are more suitable for problems of the attosecond time resolution in the electron dynamics and for studying strongly correlated motions at the length scale of 10–100 nm in solids, which are typically completely reversible. In this case, it is possible to use the high spatial coherence of single-electron sources more completely. A comparison of single-electron sources and ultrabright electron sources shows that the problem of the dynamics of chemical reactions with atomic resolution is in fact a problem of visualization with the maximum possible frame rate taking sample restrictions into account [40]. The source should have not only the sufficient spatial resolution but also the brightness and stability for achieving the maximum SNR and the maximum contrast and dynamic range for making an atomic movie as usual cameras do.

The electron scattering cross section is approximately a million times higher than that of X-rays, and therefore the time-resolved electron diffraction (TRED) method is very efficient for probing the structural dynamics of free molecules and surface layers, nanostructures, and thin films. On the other hand, X-rays, having a considerably lower scattering cross section, can penetrate into materials a few orders of magnitude more deeply than electrons. Therefore, X-rays are more convenient in practice for studying crystalline and liquid samples a few tens of micrometers in thickness. Indeed, with the development of X-ray synchrotron sources and XFELs, which can generate high radiation densities, time-resolved X-ray diffraction (TRXD) methods can become a general and powerful tool for studying the structural dynamics of matter, primarily in the condensed state. At present, these methods are being successfully used to study the dynamics of chemical and biological systems [45, 60–75].

An alternative method of electron imaging of the reaction dynamics is Rydberg spectroscopy [76]. The focus of the discussion here was the interaction of a free electron with a molecular ensemble for simulating the molecular dynamics in gas and condensed phases. Coulomb interactions between a moving electron and the complex electrostatic potential of a molecule produce phase shifts in the electron wave function. During diffraction of electrons, these phase shifts are projected on a distant detector and are observed as a diffraction pattern.

The electron wave functions can also be used to observe the structural molecular dynamics by the behavior of outer electrons in Rydberg states. As in the case of freely moving electrons, the stationary wave functions of Rydberg electrons experience phase shifts caused by Coulomb interactions with all nuclei and electrons of the molecular system. Therefore, the binding energy of a Rydberg electron to the nucleus of a molecular ion depends on the molecular structure, as shown in Fig. 2 [76–79]. Measurement of the binding energy of Rydberg ions can hence be used as a method of structural spectroscopy. Because orbital periods for Rydberg states with moderate quantum numbers are much shorter than typical time scales of the chemical dynamics, Rydberg spectroscopy can be time resolved.

The electron spectroscopy of Rydberg states can be used for measurements of the structural dynamics because the size of Rydberg orbitals exceeds that of typical molecules. Therefore, the method can be applied to both large and small molecules [79]. Because the number of Rydberg states is determined by the quantum mechanics of angular momentum states, the complexity of spectra is not scaled by the

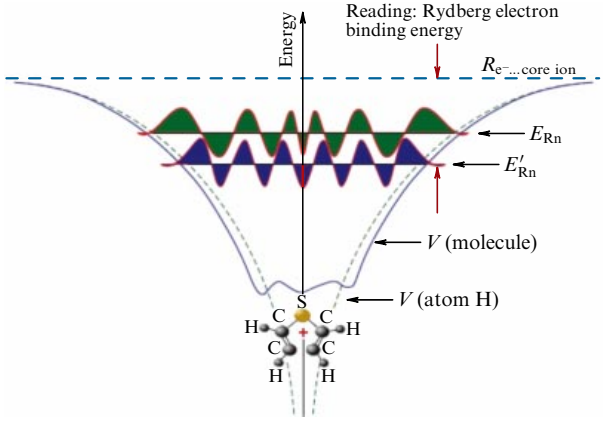

Figure 2. Rydberg electron binding energy: the energy difference between the vacuum level and the Rydberg orbital is sensitive to the structure of the molecular ion because the interaction between the Rydberg electron, nuclei, and inner electrons causes phase shifts depending on their position [78]. E_{Rn} and E'_{Rn} are the energies of Rydberg states.

molecule size. Rydberg states can exist for neutral molecules or positive-charged ions. This is explained by the fact that any positive-charged molecular ion causes the Coulomb attraction to a negative-charged electron and determines the Rydberg orbits. A chemical binding does not necessarily affect the Rydberg binding energy: even for weakly coupled van der Waals clusters, the effect of the adjacent cluster molecule can be about 0.5 eV [80], which is easily observed by the spectral method.

In some molecules, the lowest Rydberg states weakly mix with valence states, and distinct Rydberg states often begin with $n = 3$ (n is the principal quantum number). The influence of structural changes on the energy of Rydberg orbitals for such low quantum numbers is considerable, and therefore the spectral resolution provided by femtosecond lasers is already sufficient for recording even weak changes. This method was used to separate the isomer forms of molecular structures [78, 81–83]. Based on characteristic binding energies, it is possible to separate even the spectra of conformers [84], which was used for observations of the kinetics of reactions [85, 86] and the motion dynamics [86, 87] of molecular systems on the complex potential energy landscapes of conformation rearrangements.

The energy of Rydberg orbitals depends of the charge distribution in the ion core. Following the time evolution of the electron energy on Rydberg orbitals, it is possible to observe the behavior of a molecule in different charge states [88–92]. Figure 3a shows manifestations of the dynamics of conformers and charge delocalization using the example of N, N′, N″, N‴-tetramethylethylenediamine [93]. The molecule can be in the localized or charge-delocalized state with a different structure. The charge-delocalized state has a symmetric geometrical structure with the charge uniformly distributed between two equivalent nitrogen atoms of ternary amino groups. There are several nonequivalent charge-localized structures that can be identified by comparing the observed binding energies with their values calculated using the density functional theory (DFT) with the self-action correction [84].

Laser excitation transfers a molecule to one of the charge-delocalized structures, but the motion of nuclei at the subpicosecond time scale rapidly transfers the system from

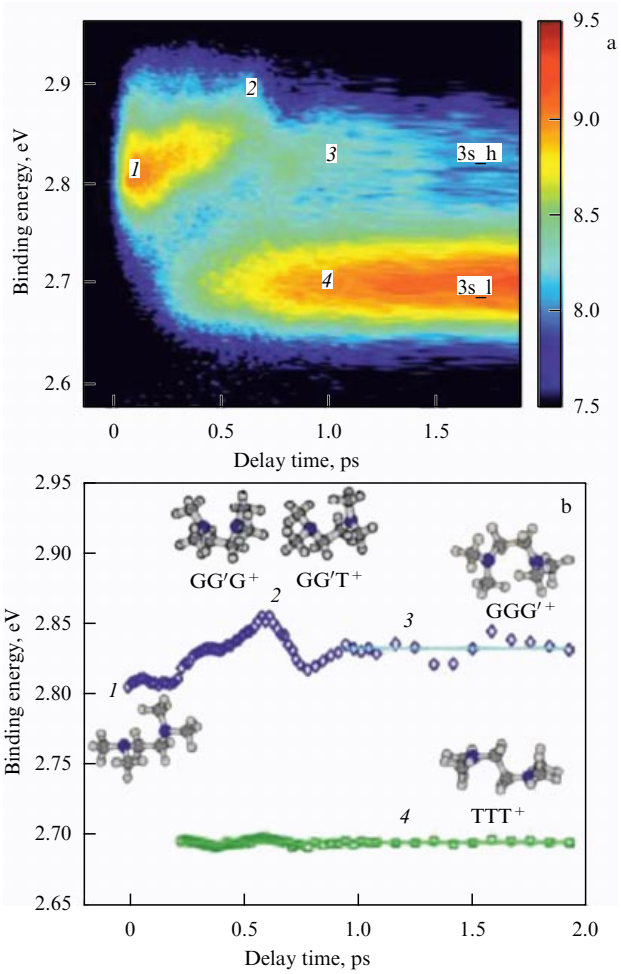

Figure 3. (Color online.) (a) Time-dependent Rydberg spectrum of N, N′, N″, N‴-tetramethylethylenediamine. Four different peaks are denoted as *1–4*: three are located in the high binding energy region and correspond to charged localized states, while the fourth peak, located at the lower binding energy, corresponds to the charge-delocalized state. (b) Centers of deconvoluted peaks with a higher binding energy (blue diamonds and line *3*) and a lower binding energy (green squares and line *4*) are respectively identified as localized and delocalized charged states. The geometry of molecular structures *1–4* leads to the appearance of spectral peaks as designated in Fig. 3a. Molecular structures are identified by gauche (*G*) and trans (*T*) positions for rotations around single bonds [93].

the region corresponding to the Franck–Condon transition to other parts of the potential energy surface corresponding to localized charge states. Some of these structures are shown in Fig. 3b. To delocalize the charge, a molecule should have a suitable geometry. This occurs during nuclear vibrations, followed by the rearrangement of electrons, which leads the system to a more stable geometry. As a result, charge delocalization occurs on the picosecond scale [88–93].

The study of the charge delocalization dynamics gives important information because laser excitation transfers molecules to nonequilibrium states. Therefore, intramolecular motions and the approach to equilibrium characterize not only the structural dynamics of the molecule but also thermodynamic parameters such as relative energy differences between different charge states. These studies were recently used to test different calculation methods [94]. It is believed that a detailed comparison of experiments with theory will provide the development of new quantum chemical methods that will better describe molecular systems, taking the possibility of charge delocalization into account.

One of the important advantages of Rydberg spectroscopy for studying variations in the molecular structure, conformation dynamics, and charge delocalization is a weak sensitivity to vibrational excitations. This is explained by the fact that the potential energy surfaces of Rydberg states for most molecules are very similar to the corresponding surfaces for ions, and hence the whole Franck–Condon envelope is located in a narrow spectral band. As a result, ionization transitions from Rydberg states are observed in the form of localized peaks, even in systems where electron transitions involving valence levels are broadened due to a strong inverse population of vibrational levels [95, 96]. Because Rydberg spectra can be measured at atmospheric pressure, this method can be used to measure intermediate structures in flames. Recently, time-resolved Rydberg spectroscopy was used to study the spatial distribution of methyl radicals in different types of flames [97].

Finally, we note that other methods exist for probing molecular structures at femtosecond time scales with the help of inner electrons. With the development of attosecond spectroscopy, it became possible to use correlations in the generation of high harmonics with respect to the formed harmonic profile for imaging the electron wave function [87]. There are many interference methods, and as a result this approach considerably depends on the theory required for relating experimental signals to the structure of molecules under study. Similarly, the high-harmonic generation by 5 fs phase-stabilized laser pulses can be used to control photoelectron emission at energies of about 100 eV, producing probe electron pulses inside a molecule itself at a wavelength of about an angstrom.

This experimental method, called laser-induced electron diffraction (LIED) [98], is similar to Rydberg spectroscopy using inner electrons to determine the molecular structure. The difference is in the much higher energy of electrons involved in LIED and hence the much shorter de Broglie wavelength. In this case, the observed signal is sensitive to vibrations and correlated nuclear motions. The energy range is almost the same as for low-energy electron diffraction (LEED).

The main difference between LIED and LEED is that the spatial coherence of the source cannot be correctly determined. This is explained by the fact that photoemission involves many e–e interactions with a scattering source (donor molecule) and accompanying correlation effects, which require the use of a complex theoretical apparatus to interpret the distribution of scattered electrons and relate it to structural changes. The required theoretical level and a nonlinear scaling of scattering terms with the number of atoms probably restrict this method to small systems. Nevertheless, the LEED method has provided images of correlated atomic motions in response to changes in the electron distribution. The main advantages of LIED are the very high time resolution and the absence of a parasitic scattering background. The main disadvantage is that measurements require strong laser fields, which significantly affect the molecular dynamics, possibly restricting the LIED applications to only photoionization-related effects [99].

The unique feature of attosecond physics is that it opens up possibilities for studying the interaction of strong electro-

magnetic fields with the prospects of controlling the ultrafast electron dynamics. In the future, these methods will give unique information for the development of a scaled time-depended *ab initio* theory for solving the problem of direct observations of the reaction dynamics with atomic resolution by using bright pulsed electron sources.

5. Ultrafast electron microscopy

Simple estimates show that the visualization of the motion of atoms in molecular and condensed systems requires resolving picometer displacements on the time scale of ~ 10 fs. The authors of [100] demonstrated the compression of single-electron pulses with the de Broglie wavelength 0.08 Å to 28 fs (FWHM), which is considerably smaller than for most of the periods of phonon vibrations in solids and normal vibrational modes of molecules.

An important problem in the field of 4D electron microscopy remains the observation of the image diffraction pattern produced by a single electron pulse, which was earlier achieved with nanosecond pulses [101]. The solution to this problem would allow the study of ultrafast irreversible processes. A breakthrough was achieved due to the collaboration of researchers from Brown University (USA) and Stanford University (USA) at the SLAC (Stanford Linear Accelerator Center) facility, where ultrashort 5.4 MeV electron pulses were used to record single diffraction patterns from 160 nm thick aluminum films [102, 103]. These studies have shown that electrons with energies of a few MeV can provide a time resolution ~ 100 fs in the single-pulse regime. Later, researchers in Japan, using a magnetic sector to compress electron bunches, obtained diffraction patterns for thin gold films from a single subpicosecond electron bunch [104].

We note in this connection that a system based on a time-of-flight reflectometer for compressing electron bunches is being developed [105]. At present, radiofrequency compression is used.

5.1 Instrument designs

High-resolution electron microscopy uses two of the main properties of the electron: a short wavelength and the presence of an electric charge, which allows controlling its motion with the help of electric and magnetic fields [17, 106–124]. In the early 1960s, a third property, the small electron mass, also found applications in so-called stroboscopic electron microscopy for studying periodic processes in samples [125].

The principle of the method is rather simple: a sample with properties periodically changing in time at a fixed frequency should be irradiated by short electron pulses at the same frequency and a fixed phase. Then the obtained image 'freezes' and thus fixes the state of the sample at the times the electron pulses arrive.

In the early 1960s, in the USSR (Spivak and co-authors [126, 127]) and other countries, stroboscopic methods were developed for all the main types of electron microscopes: transmission, scanning, emission, and mirror. These methods were used for studying rapid periodic processes in thin films (transmission microscopes) and surface layers of solids (scanning, emission, and mirror microscopes): repolarization of different ferroelectrics; features of the domain structure under remagnetization of thin magnetic films and the inhomogeneity of alternating fields of magnetic heads; local defects of p–n transitions under their rapid switching to the closed or open state; etc. [128].

The first stroboscopic electron microscope studies were performed with a micro- and nanosecond resolution, and then periodic processes were studied with a picosecond resolution in several laboratories (usually with scanning stroboscopic electron microscopes).

The main difficulties appeared during the electron-beam strobing (interruption, modulation). Commonly, one of the two methods is used: either the beam intensity is changed (the beam is locked or unlocked) when the corresponding voltage pulses are applied to the cathode or the modulator directly in the electron gun of the microscope, or the formed electron beam is deflected in an electric or magnetic field from a small transmission (rejecting) aperture. *Blanking* (locking or unlocking) pulses should be well synchronized with the frequency of signals on the sample, and their phase should be rigidly fixed, avoiding jitter.

Obviously, a longer relative duration of blanking pulses (the ratio of the period to the unlocking pulse duration) results in a better time resolution of a stroboscopic microscope, but also leads to a lower image brightness. Therefore, the optimal regime should be found in each particular case. In addition, the microscope resolution is impaired for very short unlocking pulses because of the imperfect fronts of these pulses, the appearance of chromatic aberration (in transmission microscopes), and the Boers effect [129]: the transformation of a part of the longitudinal component of the electron velocity to the transverse component caused by Coulomb repulsion.

The potential of stroboscopic electron microscopy is far from exhausted. For example, it is theoretically possible to study the microstructure of solutions (gels) in periodic Belousov–Zhabotinskii reactions, periodic sorption–desorption processes (for electrons with energies of less than 100 eV), and catalytic processes [128].

Transmission electron microscopy using many instruments was for a long time a powerful tool for studies in various fields, providing a subnanometer spatial resolution, but not the ultrashort time resolution. Optical microscopy using fluorescent labels such as green fluorescent proteins provided the visualization of *in vitro* effects [18]. However, despite the high time resolution, the spatial resolution of optical methods was usually restricted to wavelengths of 200–800 nm.

The authors of review [131] and monograph [18] described the development of respective methods of 4D dynamic transmission electron microscopy (DTEM) and ultrafast electron microscopy (UEM). Images and diffraction patterns were obtained in [131] using a 120 kV acceleration voltage for different materials (gold single crystals, amorphous carbon, and polycrystalline aluminum) and biological cells from rat intestines [132]. A strobed beam contains one electron per pulse on average, and the control dose is several electrons per $Å^2$; however, pulses are completely spatially and time controlled.

The influence of a spatial charge can be completely eliminated with the help of electron pulses containing only one electron in the limit. Zewail and his group demonstrated the efficiency of this approach [10, 131, 132] using a femtosecond master laser with a pulse repetition rate of 80 MHz to generate a current of about 500 pA, assuming about 40 electrons per pulse.

While the stroboscopic approach is restricted by repeating signals in which the train of electron pulses is stabilized in frequency and phase, the DTEM approach allows capturing images following single events [130] in the same way as Muybridge time sequences were the predecessors of real movies. We can expect that step-by-step imaging will finally result in the possibility to make long-awaited molecular films.

A complicated aspect of the DTEM design is the minimization of spatial-charge interactions between electrons to obtain a sufficient number of electrons for imaging. This is achieved with the help of a device emitting 10 ns electron pulses. Such long pulses can maintain the required number of electrons, about 10^8, for shooting with one pulse.

Recently, a compact electron source was developed for studying ultrafast electron diffraction [133]. The very compact design in combination with the small number of electrons in a bunch allows performing experiments without using a magnetic lens to collimate the electron beam.

Another important aspect of the technological progress is related to the detection of electrons transmitted through a sample.

The problem with a standard detector recording an electron image is that the detector reading should be sufficiently fast. This problem is solved with the help of a deflecting system for reading images formed by different electron beams at different parts of the detector, such that several images can be obtained with a CCD camera in the direct detection regime (without protecting the CCD detector surface) [130]. It was shown in [20, 21] that the nanosecond time resolution of the device is sufficient for studying many phenomena in material science, for example, the propagation of melting fronts during local heating. The DTEM method with a multiframe detector is also attractive, because its final aim is to record movies of single events.

The 4D UEM method was used in [134, 135] to image polycrystalline materials and single crystals (see also monograph [18]). Calibration was performed using images obtained by blocking femtosecond pulses applied to the electron microscope. In this case, the image was not observed, confirming the fact that electrons generated in the electron microscope were indeed obtained optically, while thermal electrons generated by the cathode could be disregarded [135]. The electron microscope can operate in the UEM and DTEM regimes. Studies with atomic resolution were performed with the UEM method in the diffraction regime with an intermediate lens mounted for the choice of the rear focal plane of the objective lens as an object. A 4D UEM method is being extensively developed [18, 136–142].

A picosecond time resolution is of interest for studying various laser-induced rapid processes in thin films. These include the ultrafast surface and volume dynamics in semiconductors, the generation of coherent acoustic phonons, the surface melting of nanoparticles, the nonequilibrium structural dynamics of phase transformations, and observations of the response of adsorbed molecules to the nonequilibrium structural changes of the surface [18].

Time-resolved electron diffraction can be observed, for example, with a compact femtosecond electronograph with a single magnetic lens forming a plane-parallel photoelectron beam in the sample plane. We note that a compact instrument with a 300 fs time resolution was recently developed that contained neither electron–optical lenses nor a system for radiofrequency electron-beam compression [142].

In [141], based on a commercial Hitachi H-300 electron microscope with a 75 kV acceleration voltage for continuous-regime measurements, an ultrafast transmission microscope was constructed.

A number of problems have been solved in reconstructing a commercial microscope. First and foremost, there was the problem of the input of pulsed electromagnetic radiation into the cathode region and the sample region inside the microscope column, which was not assumed by the design of industrial microscopes with a continuous electron beam, which were not intended for operation with ultrashort electron pulses.

Under conditions of the limited space in the cathode region, it is quite difficult to provide a stable overlap of the photoelectron and laser pulses close to the target in a vacuum. We recall that in pump–probe experiments, it is necessary to find the zero point of reference where pump laser pulses and probe electron pulses overlap not only in space but also in time. In the case of femtosecond laser spectroscopy, this is achieved by finding the 'coherent artifact' [141]. However, this method proves to be inapplicable to ultrafast electron microscopy, and an alternative approach to determining the zero point of reference has to be found. We note that the use of ultrashort pulses, on the one hand, provides an ultrahigh time resolution, but, on the other hand, prevents determining the spatiotemporal overlap region, especially when direct visual access to the sample inside the electron microscope column is unavailable during experiments.

A necessary condition for reliable measurements is the maintaining of the spatial overlap of the electron and light beams in the region of the target under study, which is complicated in an ultrafast transmission electron microscope by their small transverse sizes (several tens of micrometers). For the electron beam, this is caused by the aperture of the internal diaphragm, but for a laser beam inducing ultrafast phase transitions this is related to the necessity of having a high energy density ($\sim$ 1 mJ cm^{-2} or 1 eV Å^{-2} and higher). This is achieved by the tight focusing of laser pulses with pulse repetition rates in the range from tens to hundreds of kHz.

The high laser pulse repetition rate, in turn, provides the necessary SNR by using probe bunches containing small numbers of electrons. Such a solution to a technological problem allows studying samples in the nondestructive regime and decreases the electron bunch spread caused by the Coulomb repulsion of electrons. However, this approach increases the requirements for the electron detection system. In addition, it is necessary to use short exposures, which is especially important in studies of organic structures and biological objects.

The low vacuum level in a number of transmission electron microscopes ($\sim 10^{-6}$ Torr) requires solving technological problems for increasing the duration of stable electron emission from a photocathode. Under these conditions, it is necessary to select the photocathode material and to choose the optimal regime of its exposure to laser radiation in order to provide stable microscope operation during experiments. These problems were solved in [141], where the ultrafast interaction of a laser-induced plasma with a pulsed photoelectron beam was observed using the constructed setup. These experiments gave the main parameters of the probe photoelectron beam: the duration of photoelectron bunches, the average number of electrons per pulse, and the average transverse size of the pulsed electron beam in the target region.

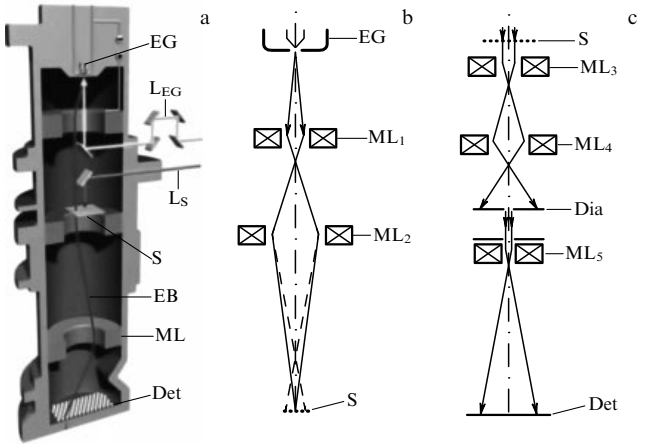

Figure 4. (a) Experimental setup of an ultrafast transmission photoelectron microscope. (b) Electron-beam and (c) sample-image formation in a Hitachi H-300 microscope. Legend: EG — electron gun, L_{EG} and L_S — laser beams irradiating the electron gun and the sample, EB — electron beam, ML — magnetic lens, ML_1 — magnetic lens of the first condenser, ML_2 — that of the second condenser, S — sample, ML_3 — magnetic lens of the objective, ML_4 — intermediate lens, Dia: diaphragm, ML_5 — projecting lens, Det — detector (fluorescent screen in the case of Hitachi H-300 before microscope reconstruction) [141].

To visualize photoelectron bunches, a 'plasma key' was developed in order to periodically change the photoelectron beam trajectory under the action of the electron cloud produced by irradiating a metal target using high-power femtosecond laser pulses. Based on the observed effect, a method was proposed for determining the zero point of reference for recording images and diffraction patterns when pump and probe pulses overlap in both space and time [141].

Figure 4a shows the fundamental setup of an ultrafast photoelectron microscope. Illustrations of the formation of the electron beam and the sample image in the microscope are shown in Figs 4b and 4c. The electron beam illumination sample is formed in two stages with the help of two magnetic condensers. The first reduces the diameter of the electron beam spot formed at the exit from the cathode unit, while the second focuses this intermediate spot image on the sample surface. Between the condensers, calibrated diaphragms can be mounted with the help of a unit in the electron microscope, which reduces the electron beam diameter and its divergence. The sample image is formed with a system consisting of one, two, or three magnetic lenses, depending on the required magnification. The image is formed on a surface covered with a luminophore and can be observed visually or recorded on a photographic plate.

The photoemission of electrons from a photocathode was excited either by the 270 nm third harmonic of a Mai-Tai, Spectra-Physics femtosecond laser or by the 263 nm fourth harmonic of an Antaus, Avesta-Proekt femtosecond fiber laser. Several metals and alloys with the electron work function smaller than the laser photon energy were tested as photocathode materials. Among the tested materials, the best results for a combination of efficiency and stability were achieved for a silver photocathode, which was used in further studies.

The authors of [141] measured the average photoelectron current in the microscope induced by laser radiation incident on the cathode. Measurements were performed by blocking the electron beam in the microscope with a Faraday cylinder and detecting a signal appearing on a resistor connected in series with the Faraday cylinder. The 4.72 eV, 300 fs fourth-harmonic pulses from a femtosecond fiber laser with a pulse repetition rate $f_L = 500$ kHz were used. For a 10 mW average radiation power, a current ~ 22 pA was measured. Taking the pulse repetition rate into account, the number of photoelectrons entering the Faraday cylinder in one laser pulse can be estimated as ~ 280, which corresponds to a photocathode quantum yield of $\sim 10^{-8}$ electrons per laser photon. We note that this quantum yield is considerably lower than the 2×10^{-5} obtained in [134, 135] for a similar cathode. Probably the quantum efficiency of photoemission in this setup strongly depends on the photocathode surface quality and the surface preparation conditions, as well as on the relatively weak vacuum in the microscope column, which differ in [141] from conditions described in [134, 135].

The insertion of a diaphragm 70 μm in diameter into the electron beam with the help of the unit in the microscope with changeable diaphragms improved the beam quality and reduced its divergence. However, the electron beam intensity in the sample region decreased by a factor of ~ 50. Nevertheless, a highly sensitive electron-counting detection system proved to be sufficient for detecting such photoelectron fluxes. Moreover, the necessary condition for achieving ultrashort photoelectron pulses is a sufficiently small number of electrons per pulse needed to reduce the pulse elongation in time caused by the Coulomb repulsion of electrons.

The initial duration of an electron bunch obtained due to photoemission from a solid cathode is determined by the time characteristics of a femtosecond laser pulse incident on the photocathode. During its propagation, a pulsed photoelectron beam is elongated in time. We discuss two main mechanisms determining this behavior.

First, the acceleration of photoelectrons in a static electric field near a cathode (up to 75 keV in [141]) elongates the electron bunch by the value of the time-of-flight chromatic aberration. For $\Delta E \approx 0.4$ eV [134, 135] and the accelerating field strength near the cathode $F \approx 3.8 \times 10^6$ V m^{-1}, this contribution is ~ 600 fs.

We note that this mechanism of the electron pulse spread, when the fast electron beam is formed due to acceleration in an electrostatic field, is not related to the Coulomb repulsion of likely charged particles. This mechanism manifests itself even in experiments with probe pulses containing several photoelectrons, for example, when a master laser with a megahertz pulse repetition rate is used, but experimental data are then averaged over many laser pulses.

To generate ultrashort photoelectron pulses with the required kinetic electron energy equal to tens or hundreds of keV, a superstrong electrostatic field can be used in the acceleration gap, and this circumstance should be taken into account in the design of an instrument operating in the ultrafast electron diffraction regime. The restriction here is a vacuum breakdown between the accelerating electrodes.

The SNR was increased by averaging over a few adjacent pixels of the image detector and accumulating a signal during the time interval corresponding to many electron beam pulses. The detector sensitivity allowed signal accumulation during the time interval in which all experimental parameters were stable. For measurements performed in [141], this time was ~ 10 min. The typical value of the average signal at the maximum brightness of the electron beam image was $\sim 10^4$ electrons at the image point for the accumulation time of 1 s. By varying the delay

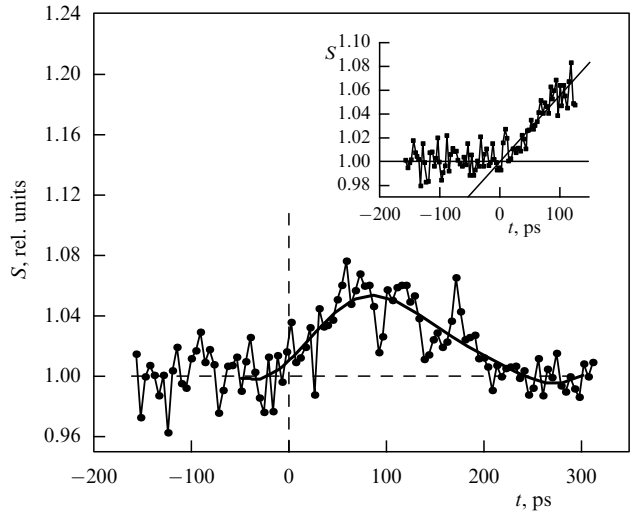

Figure 5. Dependence of the image brightness S of the electron beam of a microscope in its central part on the delay time t between a pump laser pulse and a probe electron pulse. The inset shows the time dependence of S at the initial stage of the electron beam evolution. The signal accumulation time at each point is 4 s. The solid curve shows the approximation function [141].

line length, it was possible to observe the dynamics of processes caused by the laser irradiation of the sample and affecting the electron beam in the stroboscopic regime. We note that it was found during experiments that mechanical vibrations of the laser + microscope system affect the SNR of detected signals. Therefore, to improve the SNR, it is necessary to reduce mechanical vibrations.

Figure 5 presents the dependence of the image brightness S of the electron beam in the microscope in its central part on the delay time t between the pump laser pulse and the probe electron pulse. The power density and the energy density of laser radiation in the focal spot on the sample were $\sim 2 \times 10^{10}$ W cm^{-2} and ~ 5 mJ cm^{-2}. The positive delay times in the plot correspond to the case where the probe pulse arrives at the sample after the pump pulse, while the negative delay times correspond to the pump pulse arriving after the probe pulse. Figure 5 shows that the electron-beam density in the middle part of the beam first increases for ~ 100 ps under the action of a charge 'cloud' formed near the sample surface (the propagating electron beam is slightly compressed) and then returns to the initial state.

The important parameter in the pump–probe method is the so-called 'zero point' of the time scale of experiments. This time is determined by the optical paths of the pump and probe laser beams chosen such that the beams arrive at the sample simultaneously. In the case of sample probing by photoelectrons using the method of dynamic electron microscopy, the time delay between the pump laser pulse and the probe electron pulse contains the time of flight of photoelectrons from the photocathode surface to the sample. *The delay by the electron photoemission time lies in the attosecond region* and does not therefore introduce considerable error into measurements of the coincidence time for arrivals of the electron beam and laser radiation at the target in calculations of microscopes with picosecond and femtosecond time resolutions.

The inset in Fig. 5 shows the time dependence of the signal S at the initial stage of the electron beam evolution.

A source of ultrashort photoelectron beams based on modern pulsed lasers can be used in a transmission electron microscope for observations of rapid processes induced in solids by femtosecond lasers. In the framework of this problem, a Hitachi H-300 electron microscope was modified for operation in the regime of ultrafast electron microscopy and diffraction. An ultrafast 'plasma key' based on the pulsed action of a laser plasma near a metal target on the trajectories of a sub-100 keV photoelectron beam was used to visualize the size of probe electron bunches containing ~ 300 photoelectrons: ~ 30 μm in diameter and ~ 1.4 mm in length. We note that for the same average current in the electron microscope column in the pulsed photoelectron regime, the electron concentration in the probe beam increases by $(f_L \tau_p)^{-1} \sim 10^7$ times compared to the continuous thermal emission regime [141].

5.2 Applications of time-resolved electron microscopy

Progress in the technology of ultrafast and ultrabright electron and X-ray sources made crystallographic studies at pico- and femtosecond time scales possible [142]. Advances in this field allowed observations of the structural dynamics with atomic resolution in more and more complex systems, including nonequilibrium systems in which irreversible changes occur. Making movies about the structural dynamics of nanoobjects in which irreversible dynamic processes occur is one of the most important problems in time-resolved electron microscopy.

5.2.1 Laser-induces crystallization. The authors of [101] described the observation of irreversible phase transitions caused by the rapid heating of a sample by a short laser pulse. In particular, the authors observed laser-induced crystallization in GeTe (Fig. 6). The sequence of images covers the time interval up to ~ 2.5 μs after sample irradiation. The laser

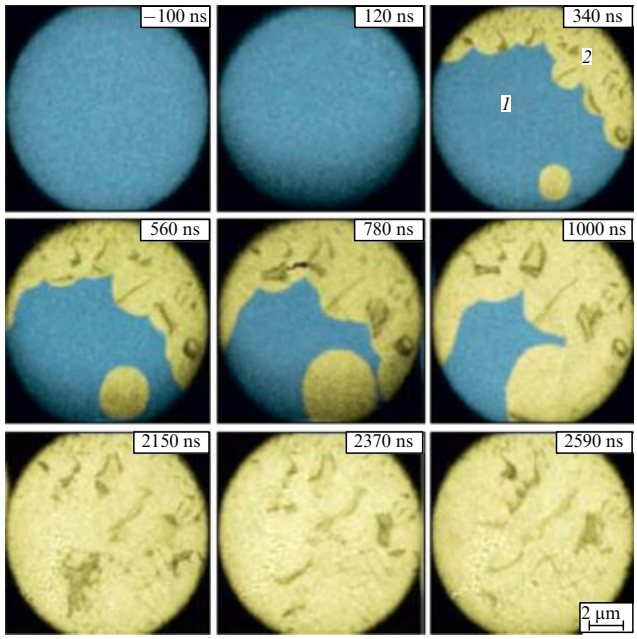

Figure 6. (Color online.) Frames illustrating the transition of amorphous GeTe (blue, *1*) to crystal regions (yellow, *2*) after irradiation using 4.7 mJ laser pulses. Separate frames were recorded using 17.5 ns electron pulses incident on different detector regions at different times, as shown in the figure.

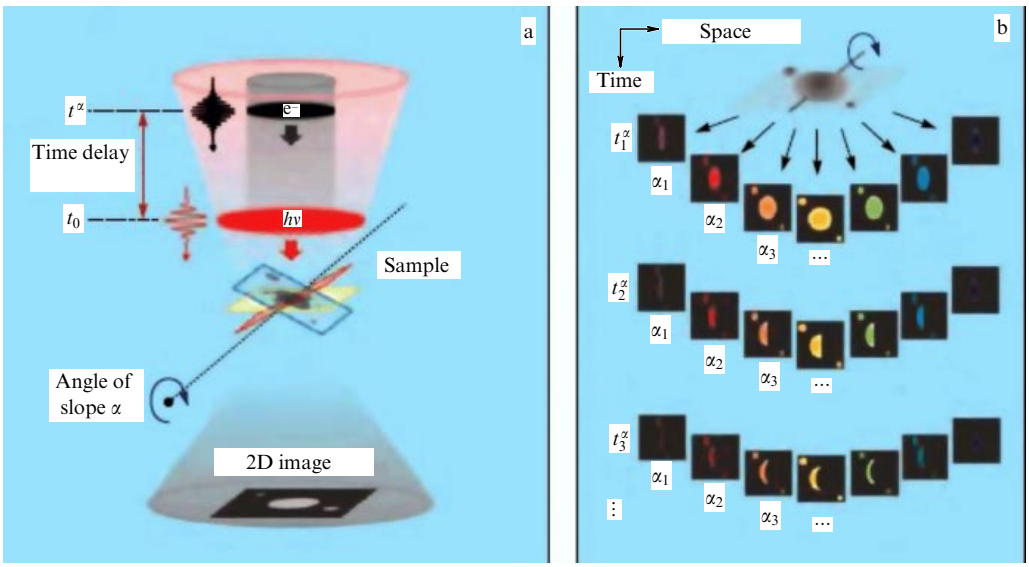

Figure 7. (a) Experimental setup of 4D electron tomography. (b) Series of two-dimensional electron images obtained at different angles α and time delays. The slope was changed from $-58°$ to $58°$ with a step of $1°$, the total number of projections reaching 4000 [144].

pulse heated the sample to a temperature above 800 K in the central part of the laser beam. The material responsed by a phase transition for a few microseconds with the formation of a crystallized GeTe. Because the microsecond time scale is much longer than the 17.5 ns electron pulse duration, each exposure 'freezes' motions in time, which allows obtaining images with good spatial resolution [101].

5.2.2 4D electron tomography. The development of electron tomography was initiated in the 1960s [143]. Progress in this area was mainly determined by the development of electronic computing tools (computers) required for processing a great number of two-dimensional electronograms and combining them.

The use of modern lasers made it possible to add time as the fourth dimension to electron tomography, thereby creating a unique instrument (Fig. 7). 4D tomography was used in [144] to study the nonstationary behavior of a carbon nanotube. The sample was twisted in the form of a bracelet. The measured nanotube length was $L \approx 4.4\,\mu$m. Photographs in Fig. 8 were made with the help of 200 keV electron pulses. Femtosecond laser excitation heated the nanotube, resulting in its structural changes, which began at the picosecond time scale. However, this attracted the special interest of a quite wide audience because of the possibility of creating a video and, in the future, a real atomic movie, using the results of 4D electron tomography. We note that the demonstration experiment in [144] did not cause irreversible changes to the nanotube structure. The total dose obtained by the carbon sample during the experiment was ~ 2 orders of magnitude lower than the dose at which the irreversible deformation of the sample could occur. This is related, in particular, to the high detection sensitivity achieved in the 4D electron microscope.

5.2.3 Plasmonics, nanophotonics, and the topological phase of matter. It is well known that the operation of almost any photonic or electronic device is based on rapidly changing electromagnetic fields. The understanding of the interaction of light with matter at the nanoscale plays a decisive role in plasmonics and nanophotonics. These fields promise advances in the computer operation rate and creation of new-generation ultrasensitive molecular biosensors.

Ultrafast electron microscopy can be used to study the internal structural dynamics, electron dynamics in the bulk, and near-field surface dynamics of photonic devices with a high spatiotemporal resolution. This gives information on the evolution of photonic phenomena [145]. The time scales of different intermediate structures found in these experiments determine a possible bound for the efficiency, which plays a decisive role for the prospects of reaching to new horizons of plasmonics and nanophotonics.

The understanding of the electron dynamics and the spatiotemporal evolution of electromagnetic fields in the bulk of materials and inside devices is a key factor in optimizing their functional efficiency. Electron microscopy can be used in principle to measure the motion of collective charge carriers and electromagnetic fields with a subwavelength resolution. In [146], a sequence of compressed 80 fs electron pulses was used for the frame-to-frame visualization of electromagnetic excitations in a metamaterial. Figure 9 shows the experimental setup used in [146].

An ultrafast electron microscope (Fig. 9) can be used to visualize electrodynamic phenomena in various miniature ultrafast devices [146]. With this method, the authors of [146] observed the motion of collective charge carriers in fields with a high spatiotemporal resolution. A collimated femtosecond photoelectron beam propagated through a metamaterial resonator excited by a one-cycle terahertz electromagnetic pulse. If the duration of the probe electron bunch is shorter than the half-period of the pump field, the Lorentz forces 'frozen' in time distort the images semiclassically. As a result, the sequence of vibrations of electromagnetic field vectors in the sample was recorded in detail, including their time, phase, amplitude, and polarization [146].

The authors of [147] studied the photoinduced electron and structural dynamics in a Bi_2Te_3 topological insulator using the methods of ultrafast electron diffraction and ultrafast IR laser spectroscopy. Such a material, characterized as a bulk insulator with surface electron conduction, was

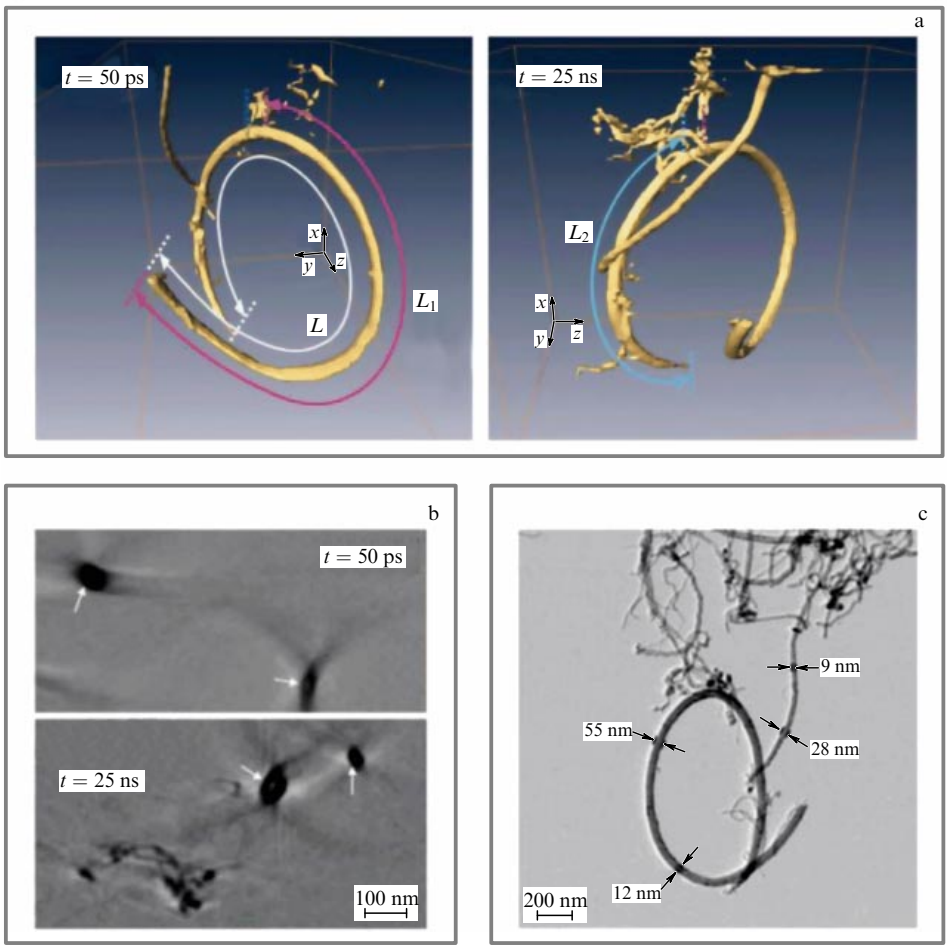

Figure 8. (a) 3D photographs of a multiwall carbon nanotube at different times. L_1 and L_2 are the lengths of corresponding segments around a fixed region. (b) The cross section of 3D images. Two-dimensional cross sections in the xy plane are shown. The cross-section thickness is 4.6 nm. Dark regions shown by arrows correspond to carbon nanometer-thick walls. As follows from the images, the spatial resolution of the method is quite sufficient for the correct imaging of channels $\sim$ 10 nm in diameter. (c) Photograph obtained with a transmission electron microscope [144].

previously studied only under conditions of applied pressure, a magnetic field, or circularly polarized light, and atomic motions and their correlation between electron systems in such solids under intense laser excitation had not been observed. It was shown in [147] that the modification of electron structures by photoinduced atomic motion in a topological insulator is a new mechanism of controlling the forbidden bandwidth. The ultrafast crystallography data show that optical excitation induces two-step atomic motion: first of bismuth and then centrally symmetric tellurium displacements. These atomic motions in Bi_2Te_3 cause a 10% narrowing of the band, in accordance with the results of ultrafast IR spectroscopy.

6. Future directions

The atomic cinema is based on a combination of spatial nanoresolution and subpicosecond or, potentially, femtosecond time resolution. We note that this is a serious challenge for most modern experimental laboratories. Therefore, a precedent in this direction plays an important role.

The idea was realized in [148] for a single metal nanostructure. A triangular silver particle 130 nm in length and 20 nm in thickness, placed on a graphene substrate (Fig. 10), was irradiated with 2.4 eV femtosecond laser pulses. Plasmon oscillations in silver excited by laser pulses were probed by an ultrashort electron beam 10 nm in diameter, which could be moved over the sample surface. In addition to spatiotemporal characteristics, an increase in the electron energy was also measured.

We emphasize that electrons not only could lose kinetic energy under the action of the field localized on a metal particle surface, as would be the case with a standard transmission microscope, but also could acquire energy [148]. This process can be controlled by tuning the laser wavelength. The accuracy is determined by the spectral width of the laser pulse and can reach $\sim$ 1 meV.

The results of measurements of a plasmon 'relief' produced on a silver surface are presented in Fig. 11. In particular, we can see that the field of plasmon oscillations excited by laser radiation is concentrated near the sharpened top of a triangle particle. Qualitatively close results were obtained near the sharp edge of copper irradiated by a laser [148].

Advances in 4D ultrafast electron microscopy in the field of nanoplasmonics and nanophotonics were used to observe the interaction dynamics of photons with matter at the atomic scale with ultrafast resolution in the image, diffraction, and energy space in [149]. In that paper, electron–photon interactions were studied using the

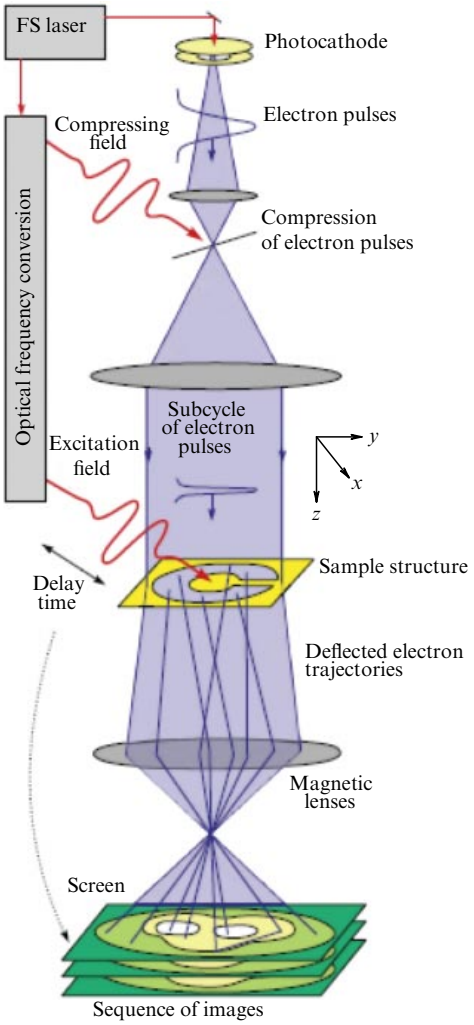

Figure 9. Concept of electromagnetic-wave electron microscopy and a diagram of the experimental setup. A femtosecond (FS) laser allows generating single-cycle terahertz pulses that locally characterize electrodynamics of the sample [146].

method of photon-induced near-field electron microscopy (PINEM) in the image and energy space. We note that the PINEM diffraction method opens the possibility of studying the structural dynamics in the inverse and energy space with ultrahigh time resolution.

Ultrafast electron microscopy makes direct observations of processes in materials in nonstationary states possible. A time resolution of the order of 100 fs corresponds to the time scale of transitions in a quantum system though the energy barrier of a potential surface and the formation or dissociation of chemical bonds in chemical reactions. Thus, advances in time-resolved electron microscopy open the possibility of studying the coherent nuclear dynamics of molecular systems and condensed matter [18, 150, 151].

During the last two decades, it has become possible to observe nuclear motion at time intervals corresponding to the nuclear oscillation period. Changes in the nuclear system during these time intervals facilitate the fundamental transition from the macroscopic kinetics of a chemical system to the dynamics of the phase trajectory of a single molecule: molecular quantum tomography [1, 13, 17, 151–153].

At present, the development of instruments and investigations of new phenomena is gaining speed. Methods of ultrafast electron crystallography and electron microscopy with time resolutions from microseconds to femtoseconds open great possibilities for studying 4D structural dynamics. Recent advances in the generation of ultrashort electron pulses allowed an attosecond time resolution for observing the coherent dynamics of electrons in molecules [154–156]. Without a doubt, remarkable events in this field are also expected in the future.

There are several research laboratories in the world that have electron microscopes operating with ultrashort electron beams and are performing or plan to perform experiments using the method of ultrafast electron diffraction. We note that the creation of a new-generation electron microscope is very important because it demonstrates the potential of leading national research centers and their capability to work at the forefront of modern science.

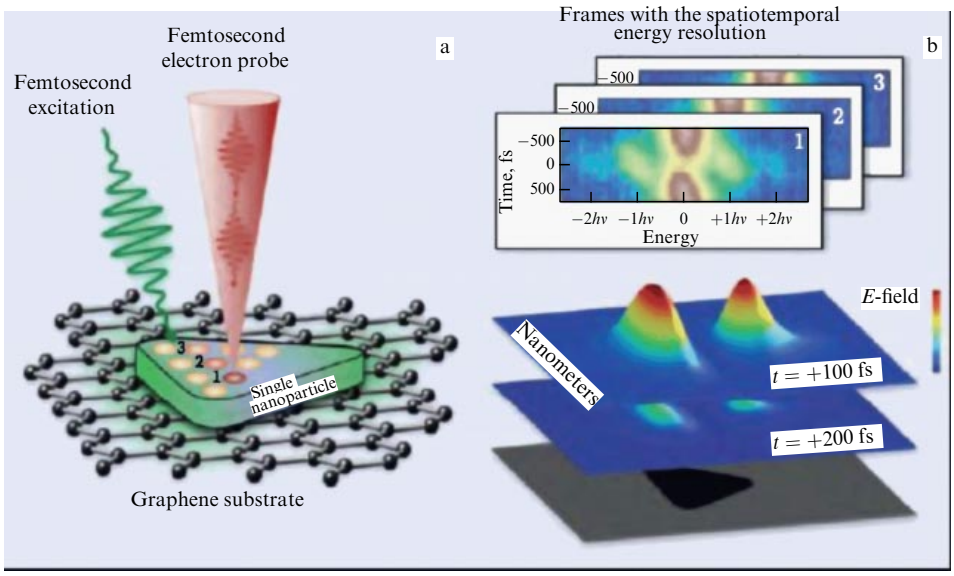

Figure 10. Process of ultrafast spectral visualization. A 10 nm electron beam scanned a silver particle preliminarily excited by femtosecond laser pulses. (a) For each position of the probe (electron bunch), electron spectra were recorded depending on the delay between the pump (optical) and probe (electron) pulses. (b) The increase in the electron energy measured in 2.4 eV laser photons [143].

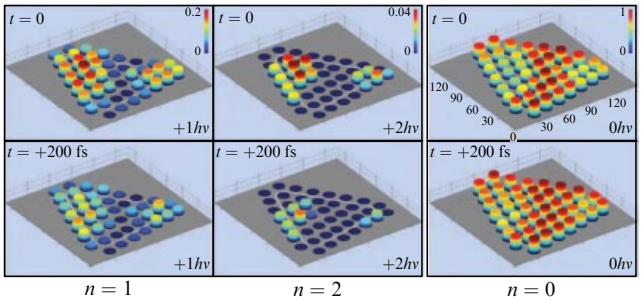

Figure 11. Visualization of photoinduced plasmon oscillations in an Ag nanostructure performed with a 10 nm electron beam. The electron signal magnitude is proportional to the height of the corresponding cylinder. The energy acquired by electrons in the interaction with nanolocalized fields is shown in the bottom right corner of each panel.

7. Conclusions

Currently, attosecond physics can provide an unprecedented time resolution and control of electron dynamics [154–156]. To spatially resolve temporal changes in the electron density in observations of time-dependent electron scattering, it is necessary to use electron probe pulses with an attosecond duration.

Ultrafast electron diffraction can be used to observe transient structures in chemical reactions and nonstationary phenomena in condensed media. However, *picosecond and femtosecond time resolutions are insufficient for studying the electron motion in atoms and molecules*. Recently, methods for generating attosecond electron pulses were proposed and experimentally demonstrated, which opens the fundamental possibility of studying the 4D coherent dynamics of electrons in molecules.

At present, ultrafast electron diffraction, crystallography, and microscopy setups, although rather complex and costly (which especially applies to ultrafast transmission electron microscopes), are already used in many scientific centers all over the world, and studies of the structural dynamics of free molecules in condensed state are rapidly being developed.

As in a number of other time-resolved measurements, attosecond experiments are often based on indirect measurements of rapid dynamics; however, they have a great potential for practical solutions to problems involving electron and nuclear dynamics. Quite reliable confirmations exist of the correct interpretation of attosecond processes by researchers as regards the measured phase shifts, distributions of arrival times, and spectral shifts in atoms, even for complex systems. Researchers are finally obtaining movies of electron charge transfer with an attosecond time resolution, and we will soon begin to understand the charge migration in large molecules using the methods of attosecond physics [157].

The first, yet rather numerous, studies in the field of attosecond physics were restricted by the use of strong near-IR fields or a combination of attosecond and femtosecond IR pulses because of the rather low intensity of subfemtosecond radiation. In the last few years, very rapid progress in increasing the energy of attosecond pulses has been unfolding in this field. The further development of this area will ensure a wider wavelength range (in the extreme UV region) and the possibility of measurements with the attosecond-pump–attosecond-probe method. Nonlinear X-ray methods will be developed for studying valence electrons and related chemical bond-formation processes [28, 158]. Coincidence methods [28] will provide new prospects for studying more complicated (multidimensional) nonlinear systems.

A combination of high-resolution spectral and diffraction methods based on various physical phenomena opens new possibilities of studying matter with the necessary integration of the structure–dynamics–function triad in physics, chemistry, biology, and material science. In the 1980s, leading research laboratories began to develop a new avenue of studies allowing the making of films on the coherent dynamics of nuclei in molecules and fast processes in biological objects — the atomic–molecular cinema.

The use of ultrashort laser pulses has drastically changed standard approaches to the study of matter with the help of electron beams and provided a high spatiotemporal resolution. The introduction of the time scan in diffraction methods, along with the development of principles of studying the coherent dynamics of atoms, has opened the way for observations of the dynamics of wave packets, the transient state of the reaction center, and electrons in molecules — *a transition from the kinetics to the dynamics of the phase trajectory of a molecule in the study of chemical reactions*.

The integration of electron optics and the pulsed laser technique in one experimental facility became an efficient method for studying the structural dynamics of matter with a high spatiotemporal resolution. This new area proved to be very promising for applications in modern physics and chemistry because studies in the 4D spatiotemporal continuum are necessary for better understanding the dynamic properties of various molecular systems with a complex potential energy surface and various phase transitions occurring in condensed media, including nanovolumes in solids.

Processes occurring in nature and technology require various instruments for their study, which, notably, is due to the duration of the processes themselves. Some characteristic time scales are presented in [159, 160]. They cover 60 orders of magnitude beginning with the Big Bang duration, the time scale of the strong nuclear interaction, and the electron rotation period around a nucleus (electron dynamics), to the age of our Universe.

The development of pulsed lasers made real-time observations of the electron dynamics possible. In fact, picosecond, femtosecond, and even subfemtosecond studies now became accessible for many applications, beginning with the recording of ultrafast processes by spectroscopic methods to the analysis of the properties of semiconductors with subpicosecond characteristic relaxation times.

Another application is so-called terahertz technology, which received a new impetus for development with the advent of high-power commercial femtosecond lasers. Also, one of the most important breakthroughs, promising for practical applications, is the discovery of the possibility of controlling chemical reactions with femtosecond resolution — photochemistry — with the use of tunable ultrashort laser pulses [161].

The development of the appropriate experimental base in the field of ultrafast electron diffraction and microscopy allowed combining a spatial resolution at the level of $\sim 10^{-2} - 10^{-3}$ Å with a picosecond and even subpicosecond time resolution. In a number of cases, the 100 fs time threshold was overcome by using 80 fs electron bunches [162–166]. With the development of this area, the generation of 10 fs pulses containing $10^4 - 10^6$ electrons would be a very

important step allowing the observation of numerous fast processes in matter and related changes in structure. In addition, it is necessary to develop an efficient method for reliable measurements of short electron bunches.

In this review, we considered processes studied with the help of modern femtosecond lasers at picosecond and femtosecond time scales and even in the subfemtosecond (attosecond) region. In this connection, the question can arise: is it possible to use ultrafast electron diffraction to study processes for very short time intervals (say, shorter than 1 as)? In principle, this can be realized using diffraction of single relativistic electrons, because they are scattered with the characteristic time $\tau = D_{\mathrm{nucl}}/c \sim 10^{-22} - 10^{-23}$ s. In our opinion, successful experiments in this field can open new possibilities for studying the dynamics of the extreme state of matter [167]. Naturally, the development of this new and promising direction will require considerable experimental and theoretical efforts (as well as significant financing of experiments). We can assume that success in this area will be determined by the efficiency of combining methods from different fields of physics, chemistry, and the latest technology in one experimental facility [168, 169].

We are presently observing, in fact, that electron microscopy, approaching the centenary of its successful development and wide applications in practice, not only is undergoing a second birth but also attains a fundamentally new level. As a result, the fundamental possibility appears of studying the properties of matter in the spatiotemporal continuum by using short photoelectron beams. The study of matter in the spatiotemporal continuum with the method of ultrafast electron diffraction opens the possibility of observing quantum phenomena in structural dynamics and in chemical reactions at the atomic–molecular level.

The main conclusion is that atomic–molecular movies can be made by using complementary information obtained in the triunity approach to this problem based on the combined use of diffraction data, spectroscopic results, and quantum chemical calculations. The many-particle potential is so complicated that the degree of nonadiabaticity of the interaction between an electron and nuclear degrees of freedom cannot be determined with the accuracy required for predicting reaction paths. A major breakthrough is the possibility of direct observations of the reaction process. How can this information and new look at the reaction dynamics be used in the future? This question arises in connection with the development of a new conceptual basis of natural sciences involving the convergence of experimental and theoretical tools for studying systems of any complexity level with an atomic resolution.

Acknowledgments

The authors thank A S Avilov (Crystallography and Photonics Research Center, RAS, P M Weber (Brown University, Providence, USA), V N Zadkov (Institute of Spectroscopy, RAS), and R J D Miller (Max Planck Institute for Structure and Dynamics of Matter, Hamburg, Germay) for the useful discussions.

The study was supported by the Russian Foundation for Basic Research (grant no. 16-29-11679 OFI_m).

References

1. Ishchenko A A, Bagratashvili V N, Avilov A S *Crystallogr. Rep.* **56** 751 (2011); *Kristallografiya* **56** 805 (2011)
2. Eigen M *Discuss. Faraday Soc.* **17** 194 (1954)
3. Zewail A H *J. Phys. Chem. A* **104** 5660 (2000)
4. Bhattacharjee Y *Nature* **412** 474 (2001)
5. Krausz F, Ivanov M *Rev. Mod. Phys.* **81** 163 (2009)
6. Sciaini G, Miller R J D *Rep. Prog. Phys.* **74** 096101 (2011)
7. Ischenko A A , Weber P M, Miller R J D *Russ. Chem. Rev.* **86** 1173 (2017); *Usp. Khim.* **86** 1173 (2017)
8. Ruan C-Y et al. *Microsc. Microanalysis* **15** 323 (2009)
9. Shorokhov D, Zewail A H *J. Chem. Phys.* **144** 080901 (2016)
10. Zewail A H *Annu. Rev. Phys. Chem.* **57** 65 (2006)
11. Dwyer J R et al. *Phil. Trans. R. Soc. A* **364** 741 (2006)
12. Srinivasan R et al. *Helv. Chim. Acta* **86** 1761 (2003)
13. Ewbank J D, Schäfer L, Ischenko A A *J. Mol. Struct.* **524** 1 (2000)
14. Miller R J D *Science* **343** 1108 (2014)
15. Ischenko A A et al. *Phys. Usp.* **57** 633 (2014); *Usp. Fiz. Nauk* **184** 681 (2014)
16. Miller R J D *Faraday Discuss.* **194** 777 (2016)
17. Ischenko A A, Weber P M, Miller R J D *Chem. Rev.* **117** 11066 (2017)
18. Zewail A H, Thomas J M *4D Electron Microscopy. Imaging in Space and Time* (London: Imperial College Press, 2010)
19. Ischenko A A, Aseyev S A (Eds) *Time-Resolved Electron Diffraction: For Chemistry, Biology and Materials Science* (Advances in Imaging and Electron Physics, Vol. 184) (San Diego: Elsevier, 2014)
20. Ischenko A A, Girichev G V, Tarasov Yu I *Difraktsiya Elektronov: Struktura i Dinamika Svobodnykh Molekul i Kondensirovannogo Veshchestva* (Structure and Dynamics of Free Molecules and Condensed Matter) (Moscow: Fizmatlit, 2012)
21. Ischenko A A *Struktura i Dinamika Svobodnykh Molekul i Kondensirovannogo Veshchestva* (Structure and Dynamics of Free Molecules and Condensed State of Matter) (Moscow: Fizmatlit, 2018)
22. Ischenko A A et al. *Appl. Phys. B* **32** 161 (1983)
23. Ischenko A A et al. *Vestn. Mosk. Univ. Ser. 2 Khim.* **26** (2) 140 (1985)
24. Akhmanov S A et al. *Sov. Tech. Phys. Lett.* **11** 63 (1985); *Pis'ma Zh. Tekh. Fiz.* **11** (3) 157 (1985)
25. Williamson S, Mourou G, Li J C M *Phys. Rev. Lett.* **52** 2364 (1984)
26. Porter G *Science* **160** 1299 (1968); Translated into Russian: *Usp. Khim.* **39** 919 (1970)
27. Demtröder W *Laser Spectroscopy* Vol. 1, 2 (Berlin: Springer, 2008)
28. Mukamel S et al. *Annu. Rev. Phys. Chem.* **64** 101 (2013)
29. Flynn G W, Parmenter C S, Wodtke A M *J. Phys. Chem.* **100** 12817 (1996)
30. Bagratashvili V N et al. *Multiple Photon Infrared Laser Photophysics and Photochemistry* (Chur: Harwood Academic Publ., 1985)
31. Akhmanov S A et al. *JETP Lett.* **26** 453 (1977); *Pis'ma Zh. Eksp. Teor. Fiz.* **26** 603 (1977)
32. Nesbitt D J, Field R W *J. Phys. Chem.* **100** 12735 (1996)
33. Letokhov V S (Ed.) *Laser Spectroscopy of Highly Vibrationally Excited Molecules* (Bristol: A. Hilger, 1989)
34. Bagratashvili V N et al. *JETP Lett.* **30** 471 (1979); *Pis'ma Zh. Eksp. Teor. Fiz.* **30** 502 (1979)
35. Makarov A A, Malinovsky A L, Ryabov E A *Phys. Usp.* **55** 977 (2012); *Usp. Fiz. Nauk* **182** 1047 (2012)
36. Li Y-L et al. *J. Org. Chem.* **67** 4228 (2002)
37. Biswas N, Umapathy S *J. Chem. Phys.* **107** 7849 (1997)
38. Kukura P et al. *Science* **310** 1006 (2005)
39. Mizutani Y, Kitagawa T *Science* **278** 443 (1997)
40. Fayer M D (Ed.) *Ultrafast Infrared Vibrational Spectroscopy* (Boca Raton, FL: CRC Press, 2013)
41. Schreier W J et al. *Science* **315** 625 (2007)
42. Asplund M C, Zanni M T, Hochstrasser R M *Proc. Natl. Acad. Sci. USA* **97** 8219 (2000)
43. Zheng J R et al. *Science* **313** 1951 (2006)
44. Cho M *Chem. Rev.* **108** 1331 (2008)
45. Chergui M, Collet E *Chem. Rev.* **117** 11025 (2017)
46. Fetisov G V *Sinkhrotronnoe Izluchenie. Metody Issledovaniya Struktury Veshchestva* (Synchrotron Radiation. Methods for Studying the Matter Structure) (Moscow: Fizmatlit, 2007); Fetisov G V *Phys. Usp.* **63** 2 (2020); *Usp. Fiz. Nauk* **190** 2 (2020)
47. Bressler C, Chergui M *Chem. Rev.* **104** 1781 (2004)
48. Ihee H *Acc. Chem. Res.* **42** 356 (2009)
49. Kim K H et al. *Nature* **518** 385 (2015)
50. Chen L X *Angew. Chem.* **116** 2946 (2004)

51. Chen L X *Angew. Chem. Int. Ed.* **43** 2886 (2004)
52. Bressler C, Abela R, Chergui M *Z. Kristallogr.* **223** 307 (2008)
53. Chen L X et al. *J. Am. Chem. Soc.* **129** 9616 (2007)
54. Gawelda W et al. *Phys. Rev. Lett.* **98** 057401 (2007)
55. Khalil M et al. *J. Phys. Chem. A* **110** 38 (2006)
56. Gawelda W et al. *J. Am. Chem. Soc.* **128** 5001 (2006)
57. Pham V-T et al. *J. Am. Chem. Soc.* **129** 1530 (2007)
58. Chen L X et al. *Science* **92** 262 (2001)
59. Altarelly M (Ed.-in-Chief), Annual Report (Hamburg: European X-Ray Free-Electron Laser Facility GmbH, 2012)
60. Coppens P *Chem. Commun.* 1317 (2003)
61. Coppens P et al. *J. Am. Chem. Soc.* **126** 5980 (2004)
62. Ihee H *Acc. Chem. Res.* **42** 356 (2009)
63. Ihee H et al. *Proc. Natl. Acad. Sci. USA* **102** 7145 (2005)
64. Kim C D et al. *Acta Cryst. A* **58** 133 (2002)
65. Techert S, Schotte F, Wulff M *Phys. Rev. Lett.* **86** 2030 (2001)
66. Schotte F et al. *Science* **300** 1944 (2003)
67. Tomita A et al. *Proc. Natl. Acad. Sci. USA* **106** 2612 (2009)
68. Šrajer V et al. *Science* **274** 1726 (1996)
69. Collet E et al. *Science* **300** 612 (2003)
70. Cavalleri A et al. *Nature* **442** 664 (2006)
71. Lee S H et al. *Phys. Rev. Lett.* **95** 246104 (2005)
72. Lindenberg A M et al. *Science* **308** 392 (2005)
73. Gaffney K J et al. *Phys. Rev. Lett.* **95** 125701 (2005)
74. Cavalleri A L et al. *Phys. Rev. Lett.* **94** 114801 (2005)
75. Fritz D M et al. *Science* **315** 633 (2007)
76. Kuthirummal N, Weber P M *Chem. Phys. Lett.* **378** 647 (2003)
77. Kuthirummal N et al. *J. Chem. Phys.* **125** 133307 (2006)
78. Gosselin J L, Weber P M *J. Phys. Chem. A* **109** 4899 (2005)
79. Liang X et al. *J. Mol. Struct.* **978** 250 (2010)
80. Gudmundsdóttir H et al. *J. Chem. Phys.* **141** 234308 (2014)
81. Deb S, Minitti M P, Weber P M *J. Chem. Phys.* **135** 044319 (2011)
82. Cardoza J D et al. *J. Electron Spectrosc. Relat. Phenom.* **165** 5 (2008)
83. Rudakov F, Weber P M *J. Chem. Phys.* **136** 134303 (2012)
84. Minitti M P, Cardoza J D, Weber P M *J. Phys. Chem. A* **110** 10212 (2006)
85. Minitti M P, Weber P M *Phys. Rev. Lett.* **98** 253004 (2007)
86. Deb S et al. *J. Phys. Chem. A* **115** 1804 (2011)
87. Bush J C, Minitti M P, Weber P M *J. Photochem. Photobiol. A* **213** 70 (2010)
88. Bush J C, Minitti M P, Weber P M *J. Phys. Chem. A* **114** 11078 (2010)
89. Cheng W et al. *J. Phys. Chem. A* **109** 1920 (2005)
90. Deb S, Cheng X, Weber P M *J. Phys. Chem. Lett.* **4** 2780 (2013)
91. Cheng X et al. *Chem. Sci.* **5** 4394 (2014)
92. Cheng X et al. *Chem. Sci.* **7** 619 (2016)
93. Cheng X et al. *J. Phys. Chem. A* **119** 2813 (2015)
94. Cheng X et al. *Nature Commun.* **7** 11013 (2016)
95. Cardoza J D, Weber P M *J. Chem. Phys.* **127** 036101 (2007)
96. Cardoza J D, Rudakov F M, Weber P M *J. Phys. Chem. A* **112** 10736 (2008)
97. Rudakov F et al. *Combust. Flame* **171** 162 (2016)
98. Niikura H et al. *Nature* **421** 826 (2003)
99. Kim J et al. *Acta Cryst. A* **66** 270 (2010)
100. Gliserin A et al. *Nature Commun.* **6** 8723 (2015)
101. Santala M K et al. *Appl. Phys. Lett.* **102** 174105 (2013)
102. Cavalieri A L et al. *Phys. Rev. Lett.* **94** 114801 (2005)
103. Hastings J B et al. *Appl. Phys. Lett.* **89** 184109 (2006)
104. Tokita S et al. *Phys. Rev. Lett.* **105** 215004 (2010)
105. Kassier G H et al. *J. Appl. Phys.* **105** 113111 (2009)
106. Hawkes P W, Kasper E *Principles of Electron Optics* Vols 1–3 (New York: Academic Press, 1996)
107. Fultz B, Howe J *Transmission Electron Microscopy and Diffractometry of Materials* (Heidelberg: Springer, 2013)
108. Parish C M, Russell P E, in *Advances in Imaging and Electron Physics* Vol. 147 (Ed. P W Hawkes) (New York: Academic Press, 2007) p. 1
109. Najafi E et al. *Ultramicroscopy* **184** 46 (2018)
110. Vainshtein B K *Sov. Phys. Usp.* **30** 393 (1987); *Usp. Fiz. Nauk* **152** 75 (1987)
111. Brandon D, Kaplan W D *Microstructural Characterization of Materials* (Chichester: J. Wiley, 1999); Translated into Russian: *Mikrostruktura Materialov. Metody Issledovaniya i Kontrolya* (Moscow: Tekhnosfera, 2004)
112. Vlasov A I, Elsukov K A, Kosolapov I A *Elektronnaya Mikroskopiya* (Electron Microscopy) (Nanoengineering Library, Book 11, Ed. V A Shakhnov) (Moscow: Izd. MGTU im. N.E. Baumana, 2011)
113. Vlasov A I, Elsukov K A, Panfilov Yu V *Metody Mikroskopii* (Microscopy Methods) (Nanoengineering Library, Book 1, Ed. V A Shakhnov) (Moscow: Moscow: Izd. MGTU im. N.E. Baumana, 2011)
114. Shindo D, Oikawa T *Analytical Transmission Electron Microscopy for Materials Science* (Tokyo: Springer-Verlag, 2002) https://doi.org/10.1007/978-4-431-66988-3
115. Umanskii Ya S et al. *Kristallografiya, Rentgenografiya i Elektronnaya Mikroskopiya* (Crystallography, Radiography, and Electron Microscopy) (Moscow: Metallurgiya, 1982)
116. Heidenreich R D *Fundamentals of Transmission Electron Microscopy* (New York: Interscience Publ., 1964)
117. Hirsch P B et al. *Phys. Today* **19** (10) 93 (1966)
118. Locquin M, Langeron M *Handbook of Microscopy* (Oxford: Butterworth-Heinemann, 1983)
119. Spence J C H *Experimental High-Resolution Electron Microscopy* (New York: Oxford Univ. Press, 1988)
120. Watt I M *The Principles and Practice of Electron Microscopy* (Cambridge: Cambridge Univ. Press, 1997)
121. Knoll M, Ruska E *Z. Phys.* **78** 318 (1932)
122. Thomas G, Goringe M J *Transmission Electron Microscopy of Materials* (New York: Wiley, 1979)
123. Amelinckx S *Methods of Direct Observation of Dislocations* (New York: Academic Press, 1964)
124. Hawkes P W *Biol. Cell* **93** 432 (2001)
125. Motosuke M, Tetsuya S "Stroboscopic scanning electron microscope", US Patent 4,538,065 (1985)
126. Spivak G V et al. *Izv. Akad. Nauk SSSR. Ser. Fiz.* **32** 1111 (1968)
127. Luk' yanov A E, Galstyan V G, Spivak G V *Radiotekh. Elektron.* (11) 2424 (1970)
128. Taheri M L, Browning N D, Lewellen J *Microsc. Microanalysis* **15** 271 (2009)
129. Knauer W *J. Vac. Sci. Technol.* **16** 1676 (1979)
130. King W E et al. *J. Appl. Phys.* **97** 111101 (2005)
131. Zewail A H *Phil. Trans. R. Soc. A* **363** 315 (2005)
132. Xia T et al. *Proc. Natl. Acad. Sci. USA* **102** 13013 (2005)
133. Badali D S, Gengler R Y N, Miller R J D *Struct. Dyn.* **3** 034302 (2016)
134. Baskin J S, Zewail A H *Comptes Rendus Phys.* **15** 176 (2014)
135. Grinolds M S et al. *Proc. Natl. Acad. Sci. USA* **103** 18427 (2006)
136. Williams J et al. *Sruct. Dyn.* **4** 044035 (2017)
137. Hassan M Th *J. Phys. B* **51** 032005 (2018)
138. Fu X et al. *Science* **355** 494 (2017)
139. Hassan M Th et al. *Nature* **530** 66 (2016)
140. Hassan M Th et al. *Nature Photon.* **11** 425 (2017)
141. Andreev S V et al. *Quantum Electron.* **47** 116 (2017); *Kvantovaya Elektron.* **47** 116 (2017)
142. Mironov B N et al. *JETP Lett.* **124** 422 (2017); *Pis'ma Zh. Eksp. Teor. Fiz.* **151** 494 (2017)
143. Frank J (Ed.) *Electron Tomography. Methods for Three-Dimensional Visualization of Structures in the Cell* (New York: Springer, 2006)
144. Kwon O-H, Zewail A H *Science* **328** 1668 (2010)
145. Barwick B, Zewail A H *ACS Photon.* **2** 1391 (2015)
146. Ryabov A, Baum P *Science* **353** 374 (2016)
147. Hada M et al. *J. Chem. Phys.* **145** 024504 (2016)
148. Yurtsever A, van der Veen R M, Zewail A H *Science* **335** 59 (2012)
149. Pomarico E et al. *ACS Photon.* **5** 759 (2018)
150. Aseyev S A, Weber P M, Ischenko A A *J. Analyt. Sci. Meth. Instrum.* **3** 30 (2013)
151. Schafer L et al. *Izv. Vyssh. Uchebn. Zaved. Khim. Khim. Tekhnol.* **60** (5) 4 (2017)
152. Ischenko A A, Tarasov Yu I, Schäfer L *Fine Chem. Technol.* **12** (4) 5 (2017); *Tonk. Khim. Tekhnol.* **12** (4) 5 (2017)
153. Ischenko A A *Phys. Res. Intern.* **2013** 236743 (2013)
154. Zheltikov A M *Sverkhkorotkie Impul'sy i Metody Lineinoi Optiki* (Ultrashort Pulses and Methods of Linear Optics) (Moscow: Fizmatlit, 2006)

155. Shao H-C, Starace A F *Phys. Rev. A* **88** 062711 (2013)
156. Shao H-C, Starace A, Madsen L, in *43rd Annual Meeting of the APS Division of Atomic, Molecular and Optical Physics, June 4–8, 2012, Orange County, CA, USA*; *Bull. Am. Phys. Soc.* **57** (5) N3.00008 (2012)
157. Leone S R et al. *Nature Photon.* **8** 162 (2014)
158. Ullrich J, Rudenko A, Moshammer R *Annu. Rev. Phys. Chem.* **63** 635 (2012)
159. Kaplan A E *Nature* **431** 633 (2004)
160. Kaplan A E *Opt. Photon. News* **17** 28 (2006)
161. Zewail A H *Nature* **412** 279 (2001)
162. Schelev M Ya *Phys. Usp.* **43** 931 (2000); *Usp. Fiz. Nauk* **170** 1002 (2000)
163. Schelev M Ya *Quantum Electron.* **41** 577 (2011); *Kvantovaya Elektron.* **41** 577 (2011)
164. Andreev S A et al. *SPIE Proc.* **6279** 62797O (2007)
165. Degtyareva V P, Monastyrskii M A, Schelev M Ya, in: Ischenko A A, Giricheva G V, Tarasiva Yu I *Difraktsiya Elektronov: Struktura i Dinamika Svobodnykh Molekul i Kondensirovannogo Sostoyaniya Veshchestva* (Structure and Dynamics of Free Molecules and Condensed State of Matter) (Moscow: Fizmatlit, 2012) p. 499, Ch. 11
166. Hansen P et al. *Appl. Phys. Lett.* **101** 083501 (2012)
167. Fortov V E *Phys. Usp.* **52** 615 (2009); *Usp. Fiz. Nauk* **179** 653 (2009)
168. Zewail A H *Acta Cryst. A* **66** 135 (2010)
169. Zewail A, Zewail M *Angew. Chem. Int. Ed.* **52** 108 (2013)